SHORT TERM SCIENTIFIC MISSION (STSM)
SCIENTIFIC REPORT

This report is submitted for approval by the STSM applicant to the STSM coordinator

Action number: TU1403-4
STSM title: Simulation and experimental analysis of adaptive component making use of PCM
STSM start and end date: 20/04/2017 to 18/07/2017
Grantee name: Stefano Fantucci

PURPOSE OF THE STSM:

The implementation in Building Performance Simulations (BPS) tools of robust models capable of simulating the thermophysical behavior of PCMs represents a fundamental step for the proper thermal evaluation of PCM components.
Reliable measuring procedures are essential to provide experimental data for validations of tools. Nevertheless, the current laboratory tests used for empirical validations of BPS presents some limitations because a small quantity of PCMs are usually exposed to conditions that are quite far from the real boundaries. Furthermore, sub-cooling and hysteresis are two features recurring in many PCM that are not currently tackled by any BPS tools. The lack of algorithms and strategies to correctly simulate these aspects can lead to wrong assumptions in designs as well as to not fully reliable findings in research and development.
The purpose of the STSM activities is to reduce the mismatch between actual and predicted thermal behaviour of PCM components through the following two actions:

- The development of accurate experimental procedure to characterise the PCM components thermal behaviour using Dynamic Heat Flow Meter Apparatus (DHFM) – (Part-A) in the following section;
- The assessment of current BPS tools and the implementation of an algorithm that account the PCM hysteresis – (Part-B) in the following section.

DESCRIPTION OF WORK CARRIED OUT DURING THE STSMS

Part (A): Experimental phase (Appendix-A) – (WG2_D2.5)
Sinusoidal response measurement procedure for thermal performance assessment of PCM by means of Dynamic Heat Flow Meter Apparatus: Data for validation of numerical models and building performance simulation tools.

Reliable and robust measuring procedures at material and at component level are essential to provide experimental data for empirical validations of software tools. Sharing of the experimental data set is also fundamental for such an activity.
The aims of the research activities were:

- to develop an experimental procedure, specifically oriented to the validation of BPS codes that implements algorithms for the simulation of PCMs, aimed at characterising and analysing the bulk-PCM thermal behaviour by means DHFM;
- to provide experimental datasets for empirical validation of BPS tools.

An experimental campaign was designed and carried out (from remote, at another lab) on two

commercially available PCM substances (PCM-a) and (PCM-b), which are representative of two different types of PCM: PCM-a is an organic paraffin based PCM (commercial name: RT 28 HC); PCM-b is an inorganic salt hydrates based PCM (commercial name: SP 26 E). The two PCMs were selected because they are characterised by different hysteresis behaviour (higher in PCM-b) and because they represent the most adopted bulk PCMs used for building envelope components.
The measurements were carried out on a polycarbonate alveolar container filled with bulk PCM.
Measurements have been conducted by means of Heat Flow Meter Apparatus for two purposes:

- To evaluate the response of PCM exposed to a sinusoidal thermal solicitation (transient state test),
- To measure the PCMs thermal conductivity in its different phases (under steady state conditions).

Prior to the experiments, transient state, 2D heat transfer analyses were carried out with a validated software tool (WUFI 2D), for numerical heat transfer simulations in order to verify the reliability the initial assumptions (i.e. dynamic equilibrium, and mono-dimensional heat transfer hypothesis) underpinning the experimental method.

Part (B): Simulation phase (Appendix-B) - (WG2_D2.4)
Modeling and empirical validation of an algorithm for simulations of hysteresis effects in Phase Change Materials for building components.

The aims of the research activities presented in this paper are:

- To empirically validate the performance of two simulation codes (EnergyPlus^{TM}, Wufi®Pro/Plus) in simulating building components implementing PCMs;
- To test the existing models (NRGSIM) for EnergyPlus that allow considering the hysteresis effect by using polynomial fitting curves method;
- To develop and validate of an algorithm that implements the hysteresis effect of PCMs by means of Energy Management System (EMS) in EnergyPlus.

The developed approach is suitable to take into consideration thermal hysteresis effect and sub-cooling effect since both can be addressed if different enthalpy vs. temperature curve can be used by the simulation tool. However, because of the lack of experimental data on sub-cooling phenomena, the verification of the proposed algorithm is only carried out for the case of hysteresis.
The performance of EnergyPlus and WUFI PCM module was compared with the experimental data without considering Hysteresis effect. Furthermore, the performance of the EMS code was verified against experimental data from DHFM apparatus.

DESCRIPTION OF THE MAIN RESULTS OBTAINED

Part (A): Experimental phase
The results of the four experimental test (two each PCM substance), carried out by DHFM apparatus are are plotted in Figure 1 and 2.

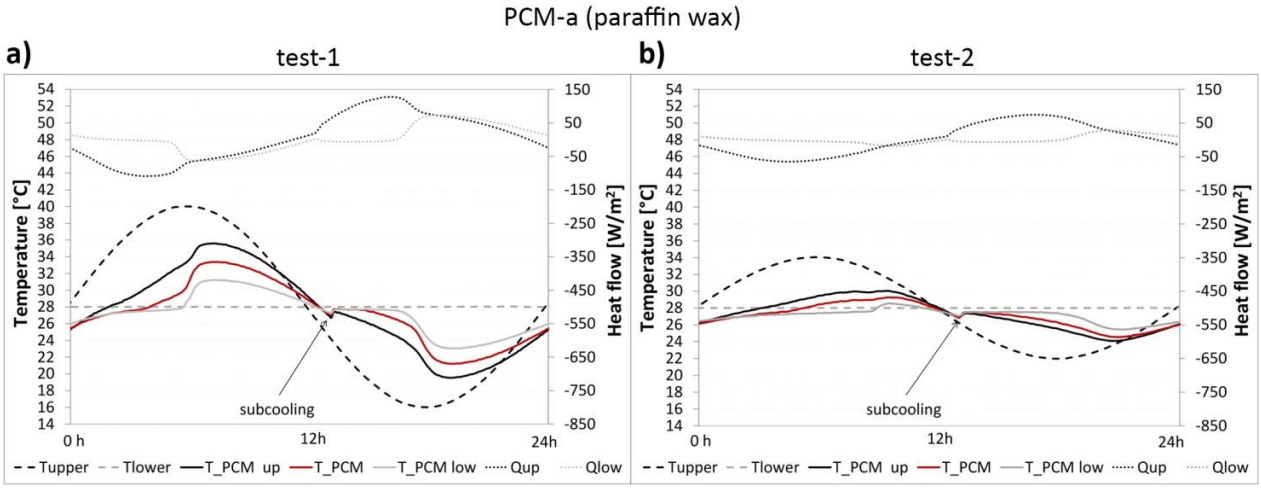

Figure 1. PCM-a (paraffin wax), experimental DHFM results: a) Test-1 (sinusoidal solicitation amplitude of 12°C); b) Test-2 (sinusoidal solicitation amplitude of 6°C).

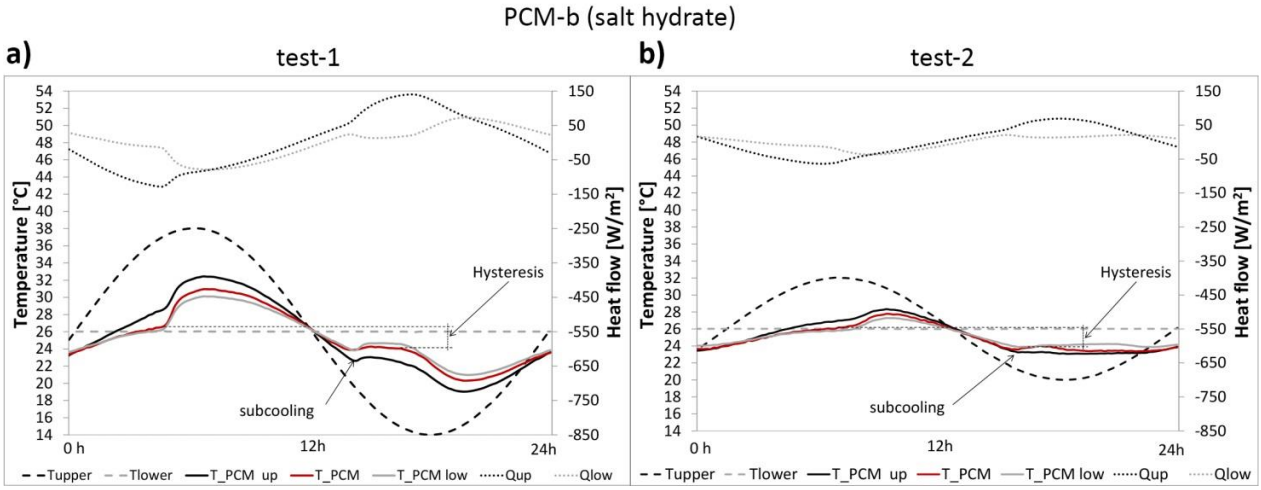

Figure 2. PCM-b (salt hydrate), experimental DHFM results: a) Test-1 (sinusoidal solicitation amplitude of 12°C); b) Test-2 (sinusoidal solicitation amplitude of 6°C).

Results are consistent with those reported in the literature regarding the behaviour of the two different PCM compositions, in particular:

- In test-1 (PCM-a and b) the change of the slope (PCM temperatures) due to the total melting and solidification of the PCMs are evident, while in test-2 (sinusoidal amplitude of 6°C), it is evident that PCM works only in their mushy state without completing the phase transition.
- As expected, salt hydrate PCM-b shows a more clear hysteresis effect (~2°C of difference between the melting and the congealing temperature) in both test 1 and 2 compared to the paraffin PCM, where this phenomenon is of little significance when the thermal stress occurs with very slow heating/cooling rates.

Furthermore, the thermal conductivity of PCM-a (paraffin wax) is strongly dependent on the PCM's state. When measured in the solid state, the thermal conductivity is 0.24 W/mK (a value coherent with those reported in the PCM datasheet), while in the liquid state the equivalent thermal conductivity is 0.4 W/mK, showing an increment of ~67%.

Part (B): Simulation phase

The simulated temperature evolution inside the PCM is represented in Fig. 3 and Fig.4, for the PCM-a "SP26E" and for the PCM-b "RT28HC". Results highlight that both EnergyPlus and WUFI are sufficiently accurate only to simulate PCM characterised by low hysteresis (organic paraffin wax) during their complete phase transitions (test-b).

The comparison between simulations and experimental data demonstrates the reliability of the proposed approach (EP_EMS) for the simulation of PCM-based components in EnergyPlus™. A slightly better match between experimental data and simulation is recorded when the new algorithm, i.e. EP_EMS is adopted compared to other approaches. Furthermore using the EP_EMS, higher improvement in the results was seen in incomplete melting conditions (tests-a).

As expected, the improvements obtained by using EP_EMS and NRGSIM are particularly important for the salt hydrate PCM-a. When the comparison is carried out with the numerical simulation that made use of the averaged enthalpy vs. temperature curve (SIM_AVG), the difference between the simulation with the proposed method and the conventional approach is less evident, yet still present.

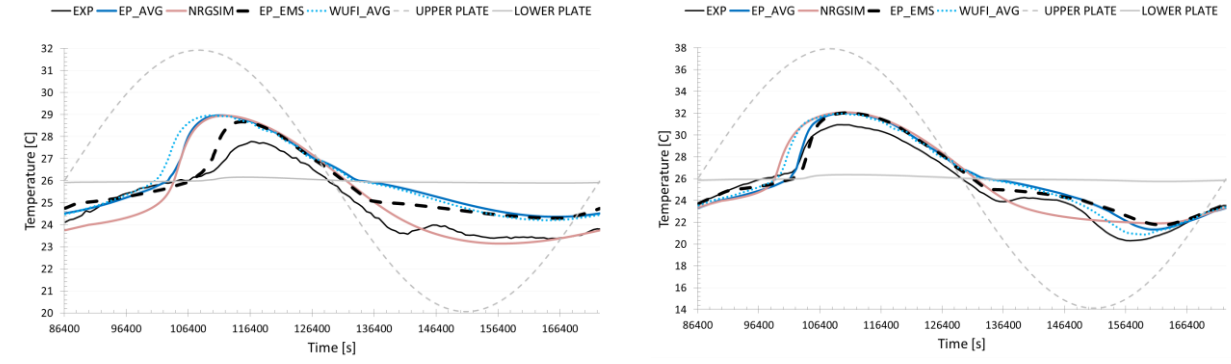

(a) **(b)**

Figure 3. Temperature evolution of SP26E under a stabilised periodic cycle. (a) Comparison between experimental data and simulations with a sinusoidal amplitude of ±6; (b) Comparison between experimental data and simulations with a sinusoidal amplitude of ±12.

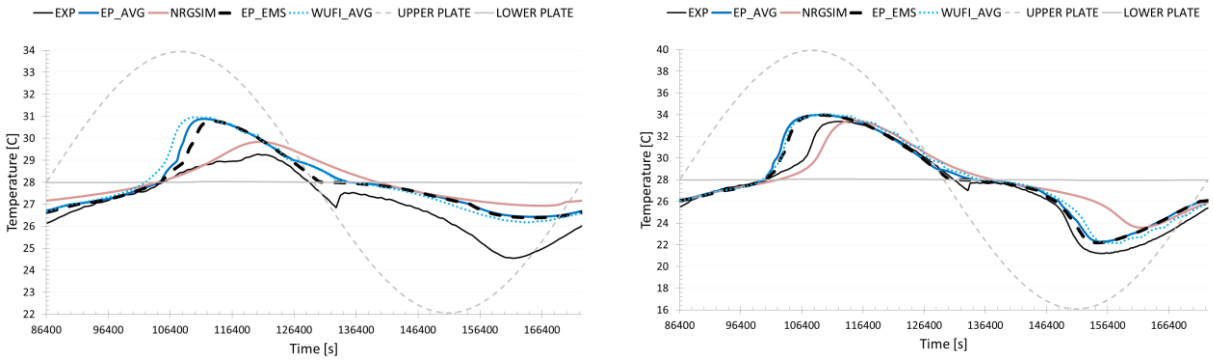

Figure 4. Temperature evolution of RT28HC under a stabilised periodic cycle. (a) Comparison between experimental data and simulations with a sinusoidal amplitude of ±6; (b) Comparison between experimental data and simulations with a sinusoidal amplitude of ±12.

FUTURE COLLABORATIONS

The developed approach to simulate hysteresis phenomena in adaptive building component implementing PCM, is also suitable to take into consideration sub-cooling effect since both the phenomena can be addressed if different enthalpy vs. temperature curve can be used by the simulation tool.
Moreover, the developed experimental procedure can be even used to perform specific experiments aimed to investigate the sub-cooling phenomena and validate numerical codes.
The above mentioned can be an input for further research collaborations in the field of simulations and experimental procedure for PCM adaptive envelope components, which are presently under discussion.

APPENDIX “A” (Paper draft)

Sinusoidal response measurement procedure for thermal performance assessment of PCM by means of Dynamic Heat Flow Meter Apparatus: Data for validation of numerical models and building performance simulation tools.

Sinusoidal response measurement procedure for thermal performance assessment of PCM by means of Dynamic Heat Flow Meter Apparatus: Data for validation of numerical models and building performance simulation tools

Stefano Fantucci[a*], Francesco Goia[b], Valentina Serra[a], Marco Perino[a]

[a] Department of Energy, Politecnico di Torino, Corso Duca degli Abruzzi 24, 10129 Torino, Italy

[b] Department of Architecture and Technology, Faculty of Architecture and Design, NTNU, Norwegian University of Science and Technology, Alfred Getz vei 3, 7491 Trondheim

* Corresponding author: Stefano Fantucci

Tel.: +39 011 0904550; fax: +39 011 0904499

E-mail addresses: stefano.fantucci@polito.it (S. Fantucci); francesco.goia@ntnu.no (F. Goia); valentina.serra@polito.it (V. Serra); marco.perino@polito.it (M. Perino)

Abstract

The implementation in Building Performance Simulations (BPS) tools of robust models capable of simulating the thermophysical behaviour of Phase Change Material (PCM) substances represents a fundamental step for the proper thermal evaluation of buildings adopting PCM-enhanced envelope components.

Reliable and robust measuring procedures at material and at component level are essential to provide experimental data for empirical validations of software tools. Laboratory tests used for the validations of models presents some limitations, because PCMs are usually subjected to conditions (temperature ramp and full transitions) that are quite far from the real boundaries faced by building components in which PCMs are applied. Furthermore, in many experimental full-scale mockups, the relatively small quantity of PCM installed ,and the combinations of many thermal phenomena, do not allow software tools to be tested in a robust way.

In this paper, an experimental procedure based on Dynamic Heat Flow Meter Apparatus to test the behaviour of PCM-enhanced building components has been developed, the procedure based on the sinusoidal response measurements has been set up specifically to provide data for a robust validation of numerical models and of BPS tools integrating PCM functionality. Moreover, general indications and guidelines to solve the some issues related to building specimen containing bulk PCM were provided, leading to a more accurate measurement of their performance and properties.

The experimental results, collected in a dataset, were obtained by two different bulk PCMs (organic and inorganic), highlighting that, for the empirical validation of simulation codes implementing PCM modelling capabilities, it is important to evaluate different PCM typologies and different thermophysical boundary conditions including (partial and full phase transitions). In fact, with test in partial phase transitions, some phenomena such as hysteresis and subcooling effect are more evident. The results related to the characterization of the thermal conductivity of paraffin based PCM show a significant variation of this property from solid to liquid state, highlighting that further investigations and improvements are needed for the measurement of the equivalent thermal conductivity in the different PCMs phases.

Keywords: Dynamic heat flow meter, phase change materials, experimental analysis, building components, building simulation, model validation

Acronyms

PCM	Phase Change Material
BPS	Building Performance Simulations
HFM	Heat Flow Meter
DHFM	Dynamic Heat Flow Meter
HVAC	Heating Ventilation and Air Conditioning
PC	Polycarbonate
IC	Initial Conditions
DSC	Differential Scanning Calorimetry

Nomenclature

T	Temperature	˚C
ΔT	Temperature difference	°C
R	Thermal resistance	m^2 K W^{-1}
φ	Specific heat flow	W m^{-2}
λ	Thermal conductivity	W m^{-1} K^{-1}
ρ	Density	kg m^{-3}
c	Specific heat	kJ kg^{-1} K^{-1}
l	Length	mm
d	Thickness	mm

1. Introduction

In the last few years, thermal energy storage in buildings has grown in popularity since several challenges related to energy conservation and building energy management can be addressed by means of this strategy. On the one hand, the increase of thermal energy storage capacity in a building is beneficial to reduce the risk of overheating and improve indoor thermal comfort conditions; on the other hand, additional important benefits are related to the reduction of the peak energy demand for space heating and cooling. Furthermore, thermal inertia can positively contribute to reducing the time mismatch between the energy demand profile and the renewable energy availability, thus increasing the rate of renewable energy use in buildings.

In this scenario, Phase Change Materials (PCMs) are since many years considered a promising solution, because of their high and selective thermal energy storage density. Nevertheless, to reach a successful use of PCMs in building components, a careful selection of the properties of the material is necessary, and the satisfactory design of PCMs-enhanced building components the use of Building Performance Simulation (BPS) is crucial. Despite BES software tools including PCM modelling capability are available since more than a decade, there are still many challenges related to accurate simulation of PCM-based components, such as the replication of some particular phenomena like hysteresis, sub-cooling, and temperature-dependent thermal conductivity.

Reliable and robust measuring procedures at material and at component level are essential to provide experimental data for empirical validations of software tools. Sharing of the experimental dataset is also fundamental for such an activity.

The aims of the study presented in this paper were:

i) to develop an experimental procedure, specifically oriented to the validation of BPS codes that implements algorithms for the simulation of PCMs, aimed at characterising and analysing the bulk-PCM thermal behaviour by means of dynamic heat flow meter apparatus;

ii) to provide experimental datasets based on the DHFM method for empirical validation of BPS.

1.1. Background on PCM measurement techniques for numerical model validation

The thermal properties of PCM related to the latent heat storage capacity are conventionally measured at material level by the following procedures:

- DSC (Differential Scanning Calorimetry approach) [1]: represent the most diffused technique, and it is based on evaluating the response of the PCM under a series of isothermal step or a dynamic temperature ramp, both in heating and cooling mode. The main limitation of this technique is that the measurement can be performed only on homogenous and small size samples. Moreover, some results can be strongly influenced by the test procedure [1] [3]. Furthermore, while results show a good agreement for enthalpy measurement in heating mode, some discrepancies were on the contrary highlighted in cooling mode measurements (IEA ANNEX 24 - 2011 [4]).
- T-History represents an alternative method to the DSC to characterize large PCM samples and can be used for measuring the thermal conductivity of the PCM too [5][6]. The method consists in recording the temperature variation during the phase transition, and to compare the results with a well-known reference material, usually distilled water. As mentioned, the main advantage respect to the DSC method is that this technique enables the characterisation of large samples and PCM-based building components[7], that are generally non-homogenous.
- DHFM (Dynamic Heat Flow Meter Apparatus): recently introduced in the ASTM C1784:2014 standard [8], is a method that can be applied to large-scale specimens (building component scale). The method needs a conventional Heat flow meter apparatus generally used for the measurement of thermal conductivity [9][10][11], but adjusted to perform dynamic ramp temperature solicitations. The temperature is changed in small steps (such as in DSC), and the resulting heat flow crossing the specimen is measured. The heat capacity is determined as the ratio between the heat flow released or absorbed by the specimen (heat flow variation) and the relative temperature increment [12].

  The main drawback is that HFM apparatus are generally built to host horizontal specimens, and the measurement on bulk PCM packed in containers may be affected by uncertainty due to the volumetric shrinkage of PCM that leads to the formation of small air volumes in the bulk material.

Material characterization alone is however not enough to validate Building Energy Simulation codes (BPS) for the simulation of PCM-enhanced building components, and experimental data in which PCM are subjected to several partial and total melting/freezing cycles, simulating as close as possible the actual operating conditions of PCM implemented on building components are necessary. For this reason, in recent years several experimental campaigns (at building component scale) had been carried out with the aim of validating physical-mathematical models implements in BPS tools, both on reduced-scale and on full-scale mock-up in laboratory conditions.

Dynamic measurements by means of hot-box apparatus are among the most common experimental activities on full-scale mockups [12],[14],[16],[17],[18],[19], and [20]. As sometimes highlighted by the same authors, most of these experiments showed some limitations: the PCM specimen's thickness was often not relevant to observe with enough precision the change of the slope of the temperature curve due to the phase transition of PCM, especially if installed in multilayer components that hide and attenuate the effect of the PCM. Moreover, as highlighted in [20], the measurements of some phenomena such as convection heat transfer could represent a not negligible source of uncertainty.

On the other hand, several studies had also been carried out on full scale experiments on outdoor test boxes [21][22] [23],[24],[25],[26],[27],[28] and on roof components [29],[30], and [31]. All these studies provide significant results since the building components were for long-term exposed to the outdoor environment (real condition). However, in these cases, not only the general drawbacks illustrated for the laboratory dynamic hot box experiments remain, but uncertainties may even increase due to the fact that the specimens are subjected to a multitude of simultaneous dynamic physical stresses that are not fully under control.

Though these studies may lead to good empirical validation of numerical models of the whole experimental set-up, including the test facility (i.e. the validation is obtained by comparison of the measured and simulated indoor air temperature), there is a high possibility that errors may mutually compensate, and it becomes hard to assess the reliability of the part of the code that simulates the PCM heat storage and transfer mechanism. Moreover, the construction of full-scale laboratory mock-up implies high cost and require long-term experimental campaign as well as the in-field experiments.

As highlighted in [32], simulations of PCMs behaviour presents several issues, since its actual thermal behaviours are poorly known. This unknowns makes most of the models suspicious to be not well tested in a robust way.
Starting from the shortcomings of current PCMs measurement techniques to support numerical models validation, an experimental procedure to test the performance of PCM-enhanced building components has been developed and presented in the next sections. This procedure has been developed specifically to provide data for a robust validation of numerical models and of BPS tools integrating PCM functionality.

2. Methods

An experimental campaign was carried on two commercially available PCM substances (PCM-a) and (PCM-b), which are representative of two different types of PCM: PCM-a is an organic paraffin based PCM (commercial name: RT 28 HC); PCM-b is an inorganic salt hydrates based PCM (commercial name: SP 26 E). The two PCMs were selected because they are characterised by different hysteresis behaviour (higher in PCM-b) and because they represent the most adopted bulk PCMs used for building envelope components. The most relevant thermophysical properties of the two PCM substances are reported in Table 1 (more detailed information can be found in [38]) while the physical properties of the materials that constitutes the multilayer experimental specimens are reported in Table 2. The measurements were carried out on bulk material, macro-encapsulated in a polycarbonate alveolar structure (as described in the coming sections).

Table 1. Thermophysical properties of the two PCMs [38].

name	commercial name	material class	melting range	congealing range	c	ρ (solid)	ρ (liquid)	λ (both phases)
			[°C]	[°C]	[kJ/kg·K]	[kg/m^3]	[kg/m^3]	[W/(m·K)]
PCM-a	RT 28 HC	Paraffin Wax	27-29	29-27	2.0	880	770	0.2
PCM-b	SP 26 E	Salt Hydrate	25-27	25-24	2.0	1500	1400	0.6

Table 2. Physical properties of each material that constitute the specimen. * PCMs properties are reported in Table 1.

layer	material	d	ρ	c	λ
		[mm]	[kg/m^3]	[J/kg/K]	[W/mK]
1	Gypsum board	12.5	720	1090	0.190
2	Polycarbonate	0.5	1200	1200	0.205
3	PCM layer*	9.0	-	-	-
4	Polycarbonate	0.5	1200	1200	0.200
5	Gypsum board	12.5	720	1090	0.190

Measurements were carried out by means of Heat Flow Meter Apparatus with two different purposes:

- To evaluate the response of PCM exposed to a sinusoidal thermal solicitation (transient state test),
- To measure the PCMs thermal conductivity in its different phases (under steady state conditions).

Prior to the experiments, transient state, 2D heat transfer analyses were carried out with a validated software tool [40][41], for numerical heat transfer simulations in order to verify the reliability the initial assumptions (i.e. dynamic equilibrium, and mono-dimensional heat transfer hypothesis) underpinning the experimental method.

2.1. DHFM: sinusoidal solicitation response measurements

The use of dynamic measurements based on sinusoidal solicitations presents some advantages compared to dynamic ramp solicitations. First, it is intrinsically closer to the real physical solicitation occurring in a building envelope (i.e. one side of the envelope is supposed to remain at constant temperature, while the other is subject to a temperature fluctuation that can be described through a sinusoidal function). Second, such an approach to material characterization may allow a direct comparison with the equivalent dynamic response (time lag and decrement factor) presented in the, EN ISO standard 13786:2007 method [33] (dynamic thermal performance of opaque building components): This calculation method, which leads to the determination of the dynamic performance of opaque building components when subject to a dynamic solicitation, is only applicable to building components realized with materials that are characterized by temperature-independent thermal properties, because of the employed numerical method (transfer function).

2.1.1. The DHFM apparatus

An Heat Flow Meter apparatus (HFM) is primarily used to determine thermal properties (thermal conductivity or thermal resistance) of a material under steady state heat flux. The apparatus is generally composed by an heating/cooling unit, heat flow meters, and temperature sensors (thermocouples) placed at the boundaries of the specimen (upper and lower plates). The measurement principle is based on the generation of a constant temperature difference (steady state conditions) between the two sides of the specimen, and on the measurement of the heat flow

density, a quantity that is inversely proportional to the specimen thermal resistance. Heat flow sensors and thermocouples are generally placed in a relatively small area compared to the total size of the heated/cooled plates, with the aim of measuring the physical quantities over an area that is not affected by edges effects, and thus presents an undisturbed mono-dimensional heat flow (the ring around the measurement area acts as a guarded area. In Figure 1, the main components of a HFM apparatus and its working principle are illustrated.

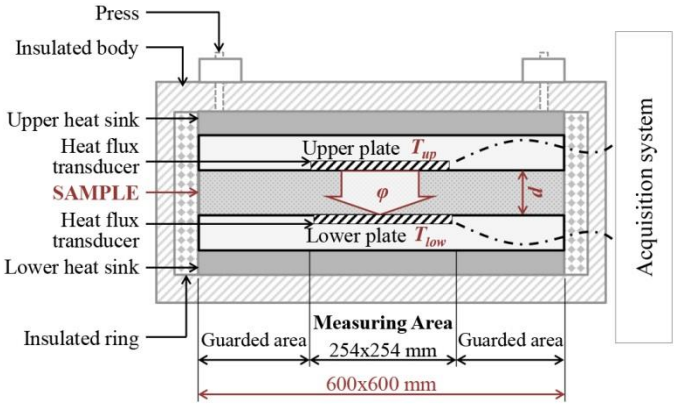

Figure 1. Heat flow meter apparatus: description and working principle.

In recent years, more advanced HFM apparatus have been produced, Dynamic Heat Flow Meter (DHFM) apparatus. These are essentially HFM apparatus with more advanced software and control unit able to perform dynamic measurements. These instruments make it possible to perform:

i) temperature ramps;
ii) sinusoidal periodic temperature solicitations.

These two measurements can be used for different purposes:

i) To measure the volumetric specific heat and enthalpy according to ASTM C1784 [8]. The principle is based on the measurement of the amount of heat absorbed/released by the specimen that, starting from an initial condition of equilibrium (steady state temperature field) is then subjected to a temperature variation. Tests are generally repeated over a series of temperature ranges. Some example of these tests are reported in [1],[12], and [34].
ii) To measure the response of a specimen subjected to a sinusoidal solicitation across a certain temperature amplitude. Generally, the characterisation is performed measuring the response in term of temperature variation of heat flow density profile on the side of a specimen subjected to a constant temperature. Some examples of these tests are reported in [3] and [35].

In the presented study the second approach based on the dynamic sinusoidal solicitation was used since the aims of the research activities are to provide a methodology and an experimental dataset specifically developed for sinusoidal solicitations, useful to test and empirically validate the capability of BPS codes to properly simulate building components implementing PCMs.

2.1.2. Materials and specimens preparation

Most of the studies reported in literature were aimed at performing experiments by means of HFM apparatus only on PCM composite systems (PCM-gypsumboards, PCM-plasters, and shape stabilized PCM in polymeric matrix), though, few studies focused on the measurements of bulk PCM (only in solid phase) can also be found [36].

The main reason for the lack of characterisations on bulk materials is that experimental measurements by means of heat flow meter apparatus when the PCM is not incorporated in a composite system but enclosed in a container presents several issues that affect the measurements:

- Difficulty in sealing the specimen (resulting in PCM sinking and loss of material);
- The volumetric heat expansion of PCM does not allow to completely fill the containers (formation of air gaps);
- Presence of thermal bridges can affect the results (metallic containers);
- Convection phenomena can occurs (if PCM is enclosed in thick containers).

For all these reasons, a new approach to perform experimental investigation on bulk PCM by means of DHFM apparatus was developed to overcome the above-mentioned issues. Such an approach is based on the use of alveolar polycarbonate containers (Figure 2), a system that presents several advantages compared to more conventional metallic containers. First, the thermal properties of polycarbonates are in the same order of magnitude of those of the PCMs (thermal conductivity of polycarbonate ranges between 0.19 – 0.22 W/mK, with a density of ~ 1200kg/m^3). Second, the alveolar structure (9x9 mm cells) reduces the convective phenomena during the liquid phase of PCM. In order to solve the issue of the volumetric expansion of the PCM, the two open sides of the specimens were folded to create an expansion vessel, and an excess of PCM was poured in the polycarbonate structure. Such a strategy allows the specimen the formation of air gaps within the measurement area to be avoided.

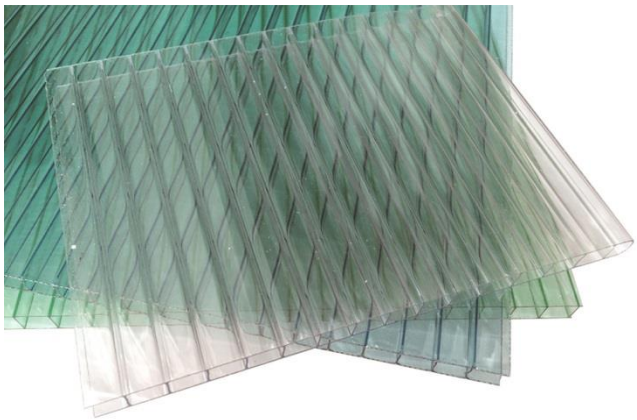

Figure 2. Polycarbonate panel used for the experiments

In Figure 3 a comparison between the procedure commonly (Fig. 3a) adopted in previous studies ([31], [36] and [37]) and the one (Fig. 3b) adopted in this study is presented. The advantages of the proposed strategy over the more conventional one can be summarised in:

- measurements without sealing the PCM's container (sealing issues and PCM leak are solved);
- all the air gaps in the specimen can be completely filled by liquid PCM;
- the excess of PCM in the expansion vessel compensates any possible decreasing of the PCM level below the upper side of the specimen during the solidification phase.

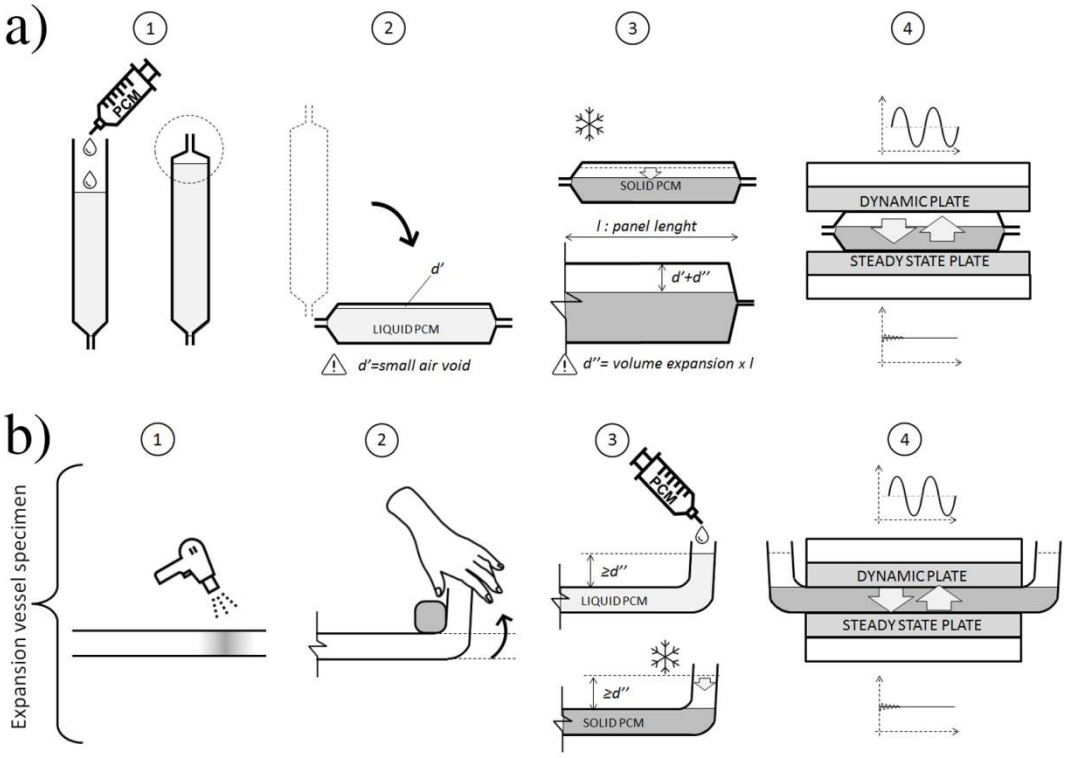

Figure 3. a) Existing procedure: (1. Vertical PCM filling and panel sealing; 2. Specimen rotation; 3. Solidification phase; 4. Measurement phase); b) Developed procedure: (1. Heat up the polycarbonate panel; 2. Fold the two sides; 3. Horizontal PCM filling; 4. Measurement phase).

2.1.3. Experimental test rig and procedure

The PCM-polycarbonate experimental specimens were sandwiched between two gypsum board panels (Figure 4) in order to avoid the direct contact between the PCM-polycarbonate specimen and the instrument plates. This solution allows the temperature in the upper and lower interface of PCM-polycarbonate specimen to be measured through external sensors, neglecting the influence of the heat flow meter apparatus plates that are maintained at controlled temperatures. Type-E thermocouples (nominal accuracy ±0.25°C), calibrated in the laboratory, were placed at the interface between the gypsum board and the PCM specimen (two thermocouples). One thermocouple was placed in the core of the PCM layer (Figure 5), inside the polycarbonate structure, with a dedicated ring surrounding the probe to assure that the temperature values were acquired at the centre of the PCM-polycarbonate specimen.

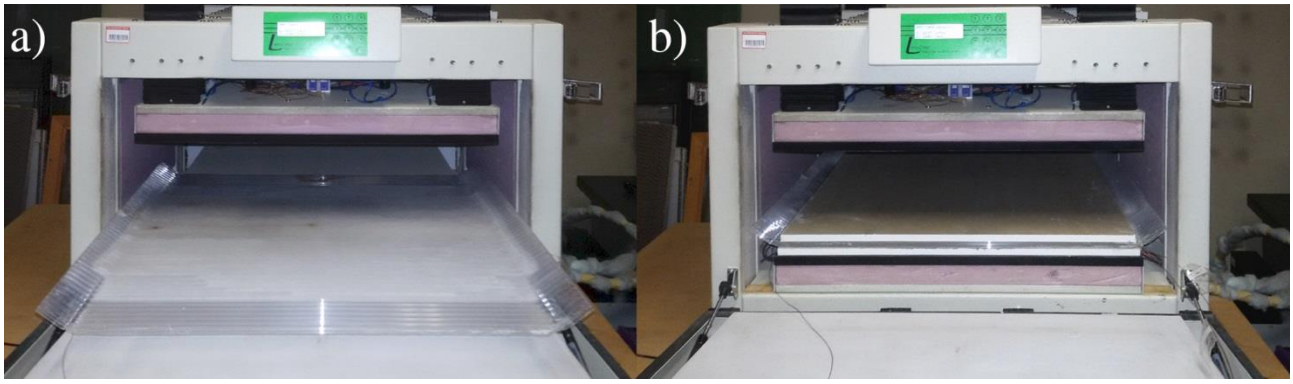

Figure 4. Preparation of the measurement specimen in DHFM apparatus. a) Placement of the PCM filled panel; b) Final overlapping by gypsum board panel.

Figure 5. Thermocouple placed in the core of the PCM layer

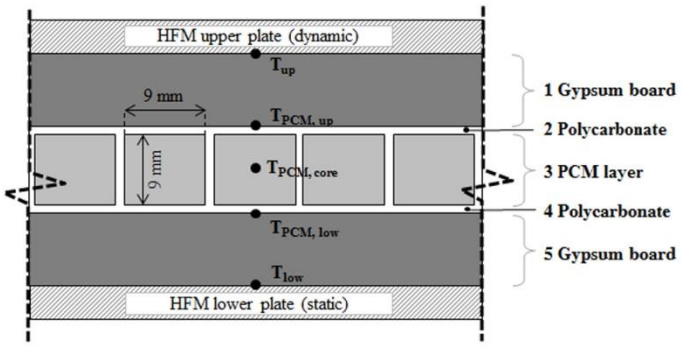

Figure 6. Layout of the measured specimen and position of the temperature sensors

The Heat Flow Meter Apparatus used in the experiment was a Lasercomp FOX600 single sample device, suitably modified to perform dynamic experiments. The device allows a 24h periodic sinusoidal temperature solicitation to be imposed on the specimen by one of the two plates while maintaining the other plate at a constant temperature. The experiments had a duration of 48h (2 x 24 h cycle), and only the results of the second cycle were stored, considering that at the second measurement cycle the dynamic equilibrium was reached. Before starting the measurement of the two cycles, an initialization period is necessary, and the dynamic cycles do not start before the set point temperature in both the instrument plates is reached. Two different tests (*test 1* and *test 2*) were carried out imposing a lower plate temperature equal to the nominal melting temperature of the PCM, and a sinusoidal upper temperature with different amplitudes, respectively ±12°C (total phase transition) for *test 1* and ±6 °C (partial phase transition) for *test 2*. The physical characteristics of each layer that constitute the measurement samples are illustrated in Table 2. Moreover, the enthalpy/temperature curve of the two PCM are illustrated in Figure 1.

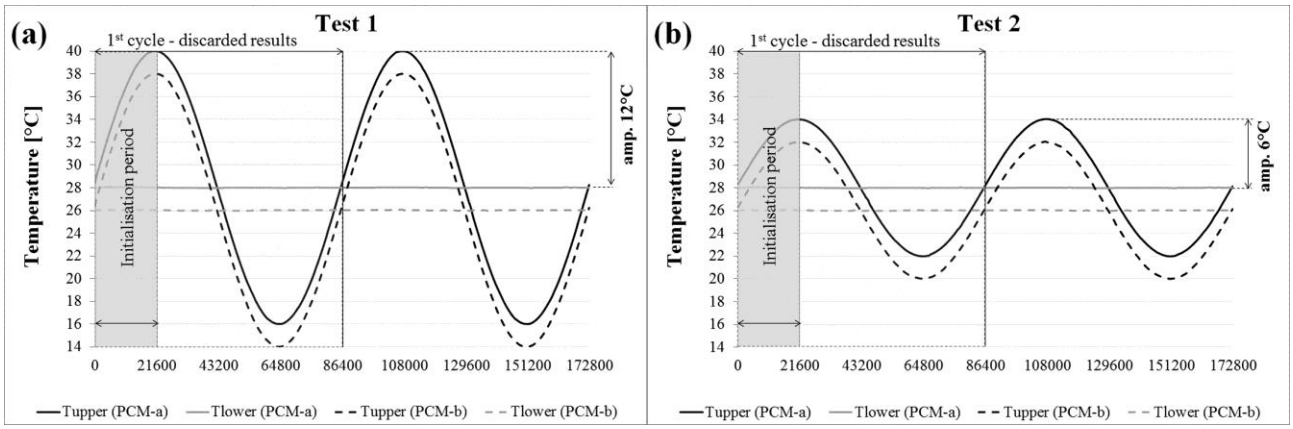

Figure 7. Measurement conditions: a) PCM-a; b) PCM-b.

2.2. Thermal conductivity measurement

The thermal conductivity of the two PCM substances was also measured by means of the same heat flow meter apparatus described in section 2.1.1, following the procedure described in EN 12664:2002 [11]. The characterization was carried out on the same samples tested with the sinusoidal response method, i.e. polycarbonate panels filled with PCM and sandwiched between two plasterboard panels.

The same instrumentation layout used in the sinusoidal response measurements was adopted, with thermocouples external to the HFM apparatus placed on the upper and lower side of the polycarbonate-PCM specimens. The measuring method is based on the one-dimensional Fourier-Biot law under steady state assumption (eq. 1):

$$\varphi = -\lambda\left(\frac{\Delta T}{d}\right) \quad (1)$$

where φ is the measured steady state heat flow through the specimen [W/m^2], λ is the sample thermal conductivity [W/mK], ΔT is the steady state temperature difference [°C] between the two sides of the specimen, and d is the thickness [m].

However, since the specimens were constituted by different layers and materials, this equation could not directly be used to evaluate the thermal conductivity of the bulk PCM alone. The indirect determination of the thermal conductivity was therefore carried out starting by the determination of the thermal resistance of the PCM layer, as the difference between the total resistance measured by the devices and the thermal resistance of the polycarbonate layers (eq. 2):

$$R_{PCM} = R_{spec.} - R_{PC} \quad (2)$$

where: R_{PCM} is the thermal resistance of the bulk PCM, R_{PC} is the thermal resistance of the two polycarbonate layers (upper PCM side and lower PCM side) and $R_{spec.}$ is the total thermal resistance of the multilayer specimen calculated as the ratio between the temperature difference ΔT measured by the upper and lower thermocouples and the measured heat flow (eq. 3).

$$R_{spec.} = \frac{\Delta T}{\varphi} \quad (3)$$

The thermal resistance of the two polycarbonate layers (upper and lower side) was determined by means of eq. (5), assuming a thermal conductivity λ_{PC} of 0.205±0.015 W/mK (as reported in the literature [39]), while the polycarbonate thickness d_{PC} was measured by means of Vernier caliper (instrumental resolution of 0.02 mm).

$$R_{PC} = \frac{2 \cdot d_{PC}}{\lambda_{PC}} \quad (4)$$

And hence the PCM thermal conductivity λ_{PCM} were determined (eq. 5).

$$\lambda_{PCM} = \frac{s - 2 \cdot d_{PC}}{R_{PCM}} \quad (5)$$

2.3. Preliminary numerical verification

Numerical heat transfer analyses were carried out to verify the following assumptions:

- Despite the alveolar geometry of the polycarbonate container, the hypothesis of mono-dimensional heat transfer is correct, and the effects of the 2D heat transfer phenomena are negligible.
- Two sinusoidal cycles of 24h each, are sufficient to assert that results were not influenced by the initial conditions.

Both the numerical analyses to verify the above-mentioned assumptions were carried out by using WUFI®2D [40], [41]. The software is a validated two-dimensional, transient heat and moisture simulation tool that solve the system of equations of heat and moisture transport using the finite volume method based on time and spatial discretization.

Building components containing PCM can be simulated assigning an enthalpy vs. temperature data in the hygrothermal function menu of the assigned PCM material.

2.3.1. Verification of measurement initialisation

One of the main drawbacks of dynamic experimental measurement is that they are usually very time consuming, and it is, therefore, important to reduce as much as possible the duration of the experiments while still maintaining an acceptable accuracy. Within the framework of this work, a numerical analysis was carried out with the aim of verifying that two sinusoidal cycles of 24h each (and thus a 48h test in total) are sufficient to achieve the stabilization of the temperature evolution during tests, when the initial conditions of the test are within a reasonable range of temperature values around the phase change range.

Before starting the experimental campaign, the assumption of the independency from the initial conditions after two sinusoidal cycles have been verified by simulating the specimen under the same sinusoidal solicitation of the DHFM analysis using different initial conditions (IC). The difference between the values of temperature of the PCM layer obtained using different IC are illustrated in Figure 8. The simulations were performed using three different IC values for the temperature of the PCM layer: 30°C (PCM in liquid phase), 28°C (PCM in melting phase), and 26°C (solid phase). As it possible to observe, in all the simulations the same value of the temperature of the PCM layer is reached after ~6h. Nevertheless to take into account that simulation software is not fully accurate for the simulation of PCMs (hysteresis phenomena and sub-cooling phenomena are not implemented), the results of the first 24 was discarded, meaning that during the second cycle (from 24th and 48th hour) the evolution of the temperature of the PCM layer is

independent from the thermal history, and the first 24 hours are sufficient as a warm up period independently from the initial temperature condition of the PCM.

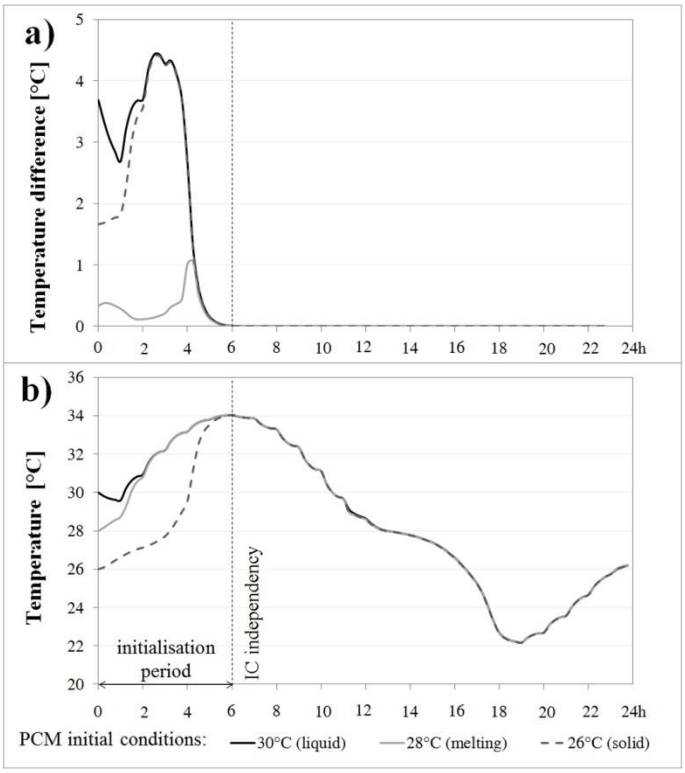

Figure 8. a) Results of the temperature difference between 1st and 2nd simulation cycle (PCM-a); b) Temperature results of the first simulation cycle (PCM-a).

2.3.2. Verification of mono-dimensional heat flow assumption

The following analysis was aimed at verifying that the effect of vertical polycarbonate structures at the boundary of each cavity of the hollow polycarbonate panel is negligible when assessing the heat transfer across the PCM layer. This assumption allows the polycarbonate-PCM system to be simplified as a homogenous layer where the heat transfer is essentially mono-dimensional.

For this verification, a 2D transient simulation was performed. To reduce the computational cost of the simulation, the heat transfer problem was simplified considering only a small portion of the specimen (30mm width) constitute by three cavities filled with PCM, which is representative of the entire structure of the sample under test.

To verify the negligibility of the 2D heat transfer, the temperature values of four sensor points (two for each side of the PCM layer) were compared. The four sensors were placed in the middle of the PCM gap and in the proximity of the vertical bridges of the polycarbonate, as shown in Figure 9. The criteria used for this verification is that the following: if the maximum temperature difference between the central sensors (T1) and the sensors placed on the sides (T2)are lower than the measurement accuracy of the thermocouples (±0.25 °C) used during the experiments, the 2D heat transfer phenomena due to the vertical bridges in the polycarbonate container can be neglected, because in practice not measurable with the test rig and procedure under investigation.

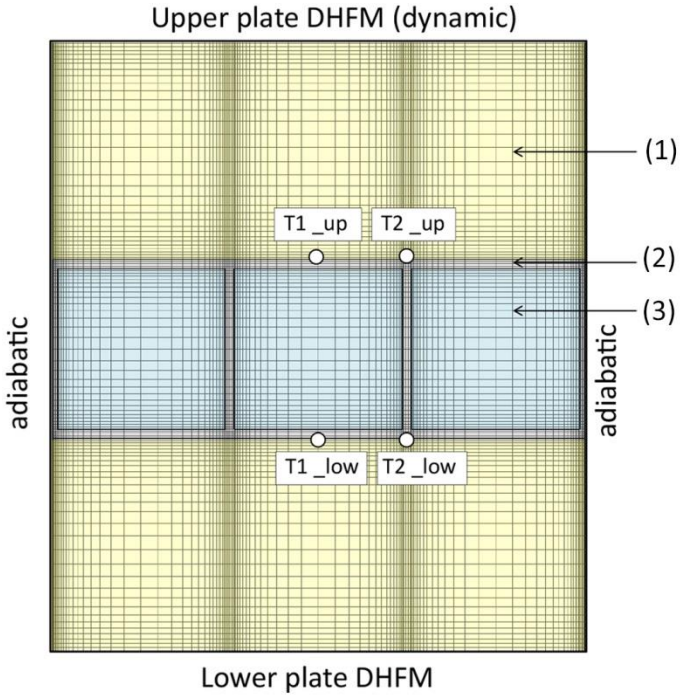

Figure 9. 2D numerical model of the measured specimen. 1) Gypsum board; 2) Polycarbonate; 3) PCM.

In Figure 10 the difference between the central temperature sensor (T1) and the temperature sensors placed on the sides (T2) are reported. The results show a maximum difference of 0.040 °C and 0.013 °C for the lower side and the upper side of the PCM layer respectively, with an associated root mean square error RMSE (between the central point and the side point) of about 0.003 and 0.002 °C. These numbers confirm that it is possible to neglect the 2D heat transfer phenomena due to the shape and the thermophysical properties of the polycarbonate container. Indeed, as already mentioned, the polycarbonate was chose as PCM container because of their similar thermal conductivities.

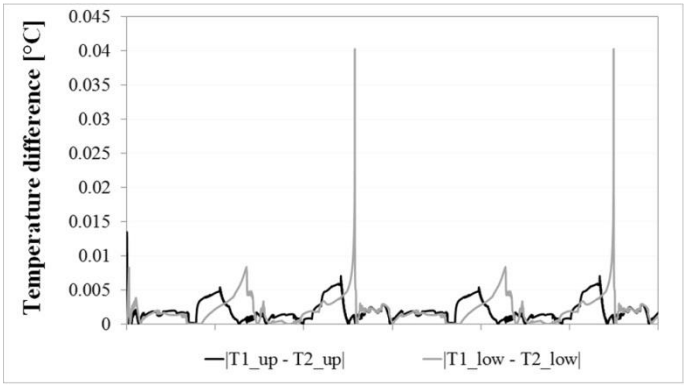

Figure 10. The difference between the control points placed in the upper and lower side of the PCM layer, simulation time 48h.

3. Results and discussion

3.1. Sinusoidal solicitation response analysis

The results of the four experimental test (two each PCM substance), carried out by DHFM apparatus are are plotted in Figure 11 and 12.

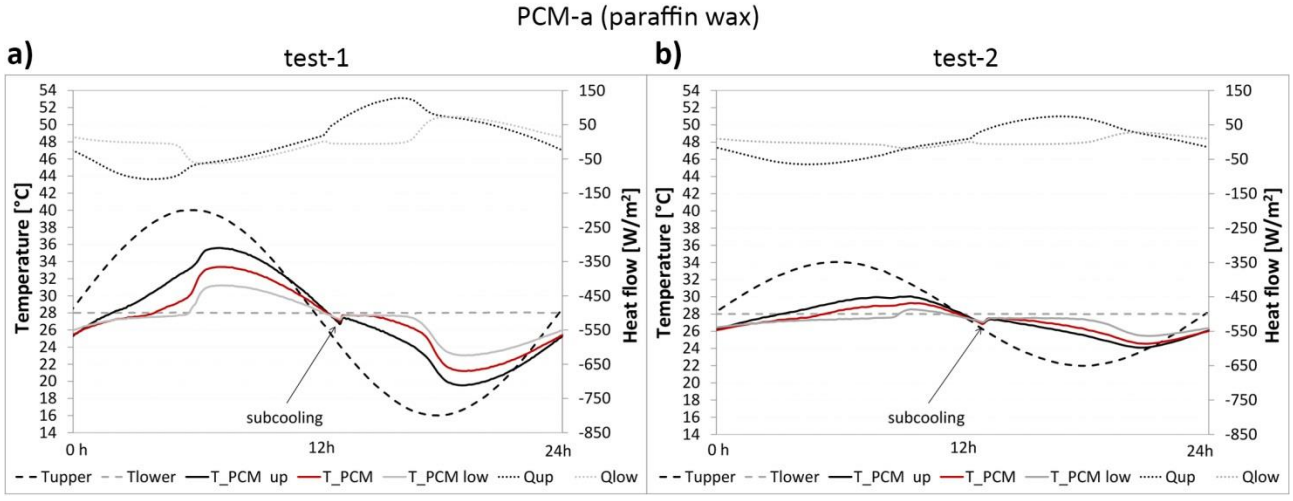

Figure 11. PCM-a (paraffin wax), experimental DHFM results: a) Test-1 (sinusoidal solicitation amplitude of 12°C); b) Test-2 (sinusoidal solicitation amplitude of 6°C).

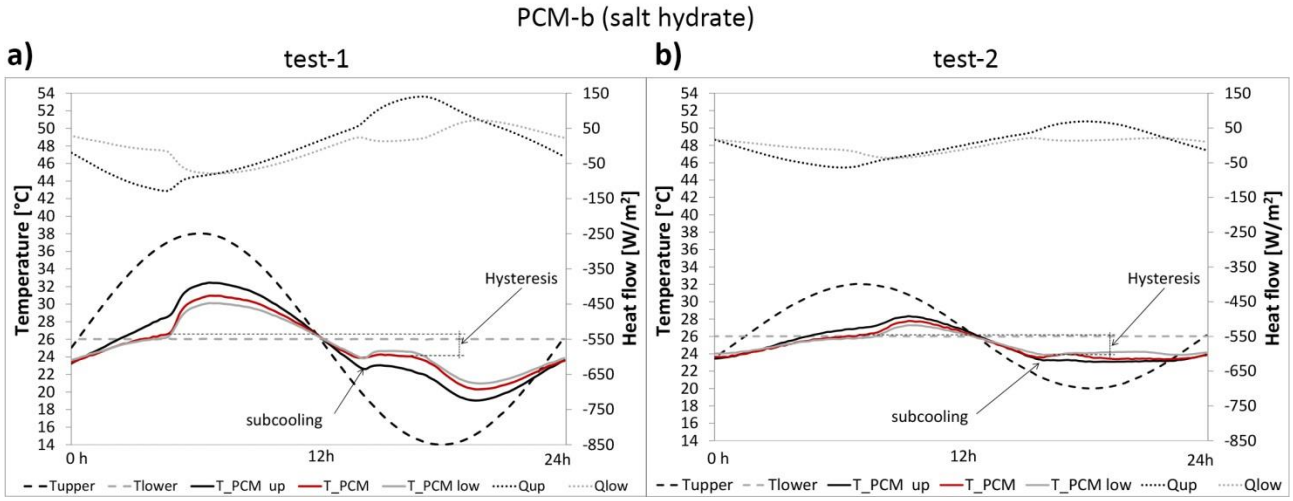

Figure 12. PCM-b (salt hydrate), experimental DHFM results: a) Test-1 (sinusoidal solicitation amplitude of 12°C); b) Test-2 (sinusoidal solicitation amplitude of 6°C).

It is possible to observe that all the results are consistent with those reported in literature regarding the behaviour of the two different PCM compositions [38], in particular:

- In test 1 (PCM-a and b) the change of the slope (PCM temperatures) due to the total melting and solidification of the PCMs are evident, while in test 2 with a sinusoidal amplitude of 6°C, it is evident that PCM works only in their mushy state without completing the phase transition.

  The relevance of these different tests, showing different behaviour of the same PCM under different boundary conditions, lays in the fact that PCM-enhanced building components are implemented in building envelope

solutions or building structures that are subjected to a wide range of thermal conditions, including both the total and the partial phase transition.

- In all the experimental results are clearly visible the sub-cooling effect. Nevertheless, it is to underline that this effect is more evident in tests 1 (complete phase transition) and in PCM-a (organic - paraffin wax).
- As expected, salt hydrate PCM-b show a more evident hysteresis effect (~2°C of difference between the melting and the congealing temperature) in both test 1 and 2 compared to the paraffin PCM, where this phenomenon is of little significance when the thermal stress occurs with very slow heating/cooling rates (lower than 0.04 ºC/min.).

In appendix A, the temperature values plotted in Fig. 11 and 12 are reported in Table 4, with a time-step of 30 minutes. The full set of experimental data containing a shorter time-step resolution, the temperatures and heat flow measured at the boundary conditions (plates), and the temperature values at the different interfaces of the samples are reported to be used for validation of software codes. Observing the relevant difference in the PCM's behaviour depending on the type of solicitation (12 ºC amplitude or 6 ºC amplitude), it is, therefore, recommendable that building simulation software tools allowing simulation of PCM substances or on-purpose developed numerical models are validated against both the tests presented in this paper. This is necessary to assure that the validation process covers a wide range of thermal conditions (more representative to the actual building operating conditions in which partial and total transition can occurs), and not only the situation when a PCM complete the heating and the cooling phase, as well as, to include in the validation phenomena such as sub-cooling and hysteresis which might be not negligible depending on the type of PCM substance (organic-inorganic).

3.2. Thermal conductivity results

Experimental results of the thermal conductivity of the PCM substances are reported in Table 3. Even though the results are affected by a relatively high uncertainty due to the indirect method of measurement leading to relevant error propagation, it is possible to observe that the following facts.

- The thermal conductivity of PCM-a (organic - paraffin wax) is strongly dependent on the PCM state. When measurement at the average temperature of 18.2°C (solid state), the thermal conductivity λ is 0.24 W/mK (a value coherent with those reported in the datasheet $\lambda_{declared}$), while at 38.7 °C (liquid state) the λ is 0.4 W/mK, showing an increment of ~67%. This difference can be justified by the possible development of convective heat transfer phenomena in the PCM in liquid phase, despite the small dimension of the cavities, and the measured value may be therefore interpreted as an equivalent thermal conductivity, which includes the contribution of another heat transfer mode that is usually neglected in PCM models for BPS tools. Because of the measurement set up, the potential convective phenomena included in the above mentioned equivalent thermal conductivity occurred under an upward heat flux. In real applications in buildings the direction of the heat flux might be different (e.g. horizontal in wall assemblies), and an investigation on these convective heat exchanges in small alveolar structures in case of different heat flux direction might be necessary to give a more robust understanding of these phenomena.
- Contrary to the organic paraffin PCM-a, PCM-b (inorganic – salt hydrate) presents a more constant value of λ for the two different phases, ~0.44 and ~0.40 W/mK, for solid and liquid phase respectively. This difference in the behaviour of the two PCMs (a and b) is probably attributable to their different compositions: in PCM-b

the presence of a salt matrix suppresses or limits to a great extent the buoyancy effects and consequently the convective heat exchange.

Despite the coherence between the results at different temperatures, it should be highlighted that in both the tests on PCM-b the resulting λ is ~ 30% ($\Delta\lambda$) lower than the value reported in the technical datasheet of the product ($\lambda_{declared}$). However this difference could be partially covered by the relatively high measurement uncertainty ($u\lambda$) of the thermal conductivity estimated in ~16% (uncertainty determined according to [42]), and by the unknown uncertainty on the declared value of the thermal conductivity.

Table 3. Thermal conductivity results λ, where T_{up}, T_{low}, T_{core} are respectively the upper, lower and core temperatures of the PCM, while $\Delta\lambda$ is the percentage difference between declared and measured values of λ.

Specimen/type	Test	T_{up} [°C]	T_{low} [°C]	T_{core} [°C]	$\lambda_{declared}$ [W/mK]	$\lambda_{measured}$ [W/mK]
PCM-a - Organic (paraffin wax)	Test 1 (solid)	16.3	21.7	18.2	0.20	0.24±0.04
	Test 2 (liquid)	37.5	41.2	38.7		0.39±0.06
PCM-b - Inorganic (salt hydrate)	Test 1 (solid)	20.9	17.3	19.0	0.60	0.44±0.07
	Test 2 (liquid)	27.0	30.6	29.2		0.40±0.06

4. Conclusion

In this paper an experimental procedure to assess the PCM thermal behaviour based on the sinusoidal response measurement with DHFM apparatus is presented, as well as, general indications and guidelines to solve the main issues related to build specimen containing bulk PCM, leading to a more accurate measurement of the PCM's performance and properties.

In order to properly measure the thermal performance of PCM layers under sinusoidal solicitations, a set of preliminary numerical analyses were carried out before the experimental activity. Results show on one hand that the polycarbonate container use to encapsulate the bulk PCM substances has a negligible effect on the heat transfer phenomena (no generation of 2D heat transfer mode) and on the other hand that two sinusoidal cycles (48h) are sufficient to measure the PCM behaviour, since after the first cycle (24h) the thermal behaviour of PCM is independent from the initial conditions of the experiment

Experimental sinusoidal response measurements on PCM substances highlight that for the empirical validation of simulation codes implementing PCM modelling capabilities it is important to evaluate different thermo-physical boundary conditions. The following guidelines should be followed:

- Results on PCM-a (paraffin wax PCM) with a complete phase transition (test 1) should be used to verify the reliability of simulation code that implements sub-cooling effect;
- Results on PCM-b (salt hydrate PCM), test 1 (complete transition) and test 2 (partial transition) should be both used to validate models that implement the hysteresis phenomena;
- Test 2 on both PCM-a and PCM-b are useful to verify the reliability of simulation code to properly simulate building component implementing PCMs under actual building thermal conditions (partial transition can frequently occur). Test 1 (PCM-a and b) are only useful to validate the capability of simulation code to properly simulate the total phase transition of PCM.

- Test on PCM-a (paraffin wax PCM) can be used to verify the codes implementing temperature dependent thermal conductivity of PCMs substances.

The authors hope that the sharing of the DHFM measurements collected in a dataset available in the Appendix and in an online repository shall be useful for the development of validated building simulations code implementing PCM modelling capability.

5. Acknowledgment

The authors want to express their gratitude to Alice Lorenzati, Rocco Costantino, and Maurizio Bressan for the helpful support during the experimental activities. Part of the research activities presented in this paper was carried out in the framework of a Short Term Scientific Mission (STSM) supported by the European Union COST Action TU1403 (Adaptive Facades Network). The authors also gratefully acknowledge the COST Action TU1403 for provided excellent scientific network.

References

[1] ASTM E793 - 06(2012 Standard Test Method for Enthalpies of Fusion and Crystallization by Differential Scanning Calorimetry

[2] Kosny, Jan; Stovall, Therese K; Yarbrough, David W. Dynamic Heat Flow Measurements to Study the Distribution of Phase-Change Material in an Insulation Matrix. 30th International Thermal Conductivity Conference, Seven Springs, PA, USA, (2009)

[3] Cascone Y., Perino M., Estimation of the thermal properties of PCMs through inverse modelling. Energy procedia, 78 (2015), 1714 – 1719.

[4] IEA (2011) Development of a test-standard for PCM and TCM characterization part 1: characterization of phase change materials. Technical report. IEA—Solar Heating and Cooling/ Energy Conservation through Energy Storage programme—Task 42/Annex 24: Compact Thermal Energy Storage: Material Development for System Integration. http://www.iea-eces. org/files/a4.3.a2_appendix_wga2_1.pdf

[5] Zhang YP, Jiang Y, Jiang Y. A simple method, the T-history method, of determining the heat of fusion, specific heat and thermal conductivity of phase-change materials. Measur Sci Technol 1999;10:201-5.

[6] Marín JM, Zalba B, Cabeza LF, Mehling H. Determination of enthalpy-temperature curves of phase change materials with the temperature history method: improvement to temperature dependent properties. Measur Sci Technol 2003;14:184-189.

[7] Kosny, Jan, PCM-enhanced building components, An Application of Phase Change Materials in Building Envelopes and Internal Structures. Springer (2015). doi: 10.1007/978-3-319-14286-9.

[8] ASTM C1784:2014, Standard Test Method for Using a Heat Flow Meter Apparatus for Measuring Thermal Storage Properties of Phase Change Materials and Products.

[9] ASTM C518:2010, Standard Test Method for Steady-State Thermal Transmission Properties by Means of the Heat Flow Meter Apparatus

[10] EN ISO 12667:2001, Thermal performance of building materials and products - Determination of thermal resistance by means of guarded hot plate and heat flow meter methods - Products of high and medium thermal resistance

[11] UNI EN 12664:2001, Thermal performance of building materials and products - Determination of thermal resistance by means of guarded hot plate and heat flow meter methods- Dry and moist products of medium and low thermal resistance

[12] Shukla N, Kosny J. DHFMA Method for Dynamic Thermal Property Measurement of PCM-integrated Building Materials. Curr Sustainable Renewable Energy Rep (2015) 2:41–46

[13] Cao S, Gustavsen A, Uvsløkk S, Jelle BP, Gilbert J, Maunuksela J. The effect of wall-integrated phase change material panels on the indoor air and wall temperature - hot box experiments. In: Proceedings of renewable energy research conference (2010), Trondheim, Norway, 7–8 June

[14] Haavi, T, Gustavsen A, Cao S, Uvsløkk S, Jelle B.P. Numerical Simulations of a Well-Insulated Wall Assembly with Integrated Phase Change Material Panels - Comparison with Hot Box Experiments," The International Conference on Sustainable Systems and the Environment (2011), Sharjah, United Arab Emirates.

[15] Kośny J, Kossecka E, Brzezinski A, Tleoubaev A, Yarbrough D. Dynamic thermal performance analysis of fiber insulations containing bio-based phase change materials (PCMs). Energy Build 52 (2012), 122–131.

[16] Kossecka E, Kośny J. Hot box testing of building envelope assemblies; a simplified procedure for estimation of minimum time of the test. J Test Eval (JTE) 36 (2008).

[17] Kośny J, Yarbrough DW, Miller W, Childs P, Syed AM (2007b) Thermal performance of PCM-enhanced building envelope systems. In: Proceedings of X conference - thermal performance of the exterior envelopes of buildings (2007), Clearwater, Florida.

[18] Kuznik F, Virgone J, Noel J. Optimization of a phase change material wallboard for building use. Appl Therm Eng 28 (2007), 1291–1298.

[19] Kuznik F, Virgone J, Experimental investigation of wallboard containing phase change material: Data for validation of numerical modeling, Energy and Buildings 41 (2009), 561-570, https://doi.org/10.1016/j.enbuild.2008.11.022

[20] Kuznik F, Virgone J, Johannes K Development and validation of a new TRNSYS type for the simulation of external building walls containing PCM. Energy Build 42 (2010), 1004–1009.

[21] Medina MA, Stewart R. Phase-change frame walls (PCFWs) for peak demand reduction, load shifting, energy conservation and comfort. In: Proceedings of Sixteenth symposium on improving building systems in hot and humid climates (2008), Plano, TX.

[22] Medina MA, Zhu D. A comparative heat transfer examination of structural insulated panels (SIPs) with and without phase change materials (PCMs) using a dynamic wall simulator. In: Proceedings of Sixteenth symposium on improving building systems in hot and humid climates (2008), Plano, TX.

[23] Khudhair AM, Farid MM. Use of phase change materials for thermal comfort and electrical energy peak load shifting: experimental investigations. In: Goswami DY, Zhao Y (eds) Solar world congress 2007. Solar Energy and Human Settlement (2007), Beijing, China.

[24] Tardieu A, Behzadi S, Chen J, Farid M (2011) Computer simulation and experimental measurements for and experimental PCM-impregnated office building. In: Proceedings of building simulation 2011: 12th conference of international building performance simulation association (2011), Sydney.

[25] Cabeza L, Castellon C, Nogues M, Medrano M, Leppers R, Zubillaga O. Use of microencapsulated PCM in concrete walls for energy savings. Energy Build 39 (2007), 113–119.

[26] Castell A, Medrano M, Castellón C, Cabeza LF. Analysis of the simulation models for the use of PCM in buildings. In: Proceedings of Effstock 2009 - the 11th international conference on thermal energy storage (2009), Stockholm, Sweden.

[27] Castell A, Martorell I, Medrano M., Pérez G, Cabeza L.F. Experimental study of using PCM in brick constructive solutions for passive cooling, Energy and Buildings 42 (2010), 534–540.

[28] Castellón C, Medrano M, Roca J, Cabeza L, Navarro M, Fernández A, Lázaro A, Zalba B. Effect of microencapsulated phase change material in sandwich panels. Renew Energy 35 (2010), 2370–2374

[29] Miller WA, Karagiozis A, Kośny J, Shrestha S, Christian J, Kohler C. Demonstration of four different residential envelopes. In: Proceedings of ACEEE Summer study on energy efficiency in building (2010), Pacific Grove, California.

[30] Kośny J, Miller W, Zaltash A Dynamic thermally disconnected building envelopes—a new paradigm for walls and roofs in low energy buildings. In: Proceedings of DOE, ASHRAE, ORNL Conference—thermal envelopes XI—thermal performance of the exterior envelopes of buildings (2010), Clearwater, Florida.

[31] Elarga H, Fantucci S, Serra V, Zecchin R, Benini E. Experimental and numerical analyses on thermal performance of different typologies of PCMs integrated in the roof space, Energy and Buildings (2017), https://doi.org/10.1016/j.enbuild.2017.06.038.

[32] Dutil Y, Rousse D, Lassue S, Zalewski L, Joulin A, Virgone J, Kuznik F, Johannes K, Dumas J.P, Bédécarrats J.P, Castell A, Cabeza L. F. Modeling phase change materials behavior in building applications: Comments on material characterization and model validation, Renewable Energy 61 (2014), 132-135.

[33] EN ISO 13786:2007. Thermal performance of building components - Dynamic thermal characteristics - Calculation methods.

[34] Ruuska T, Vinha J, Kivioja H. Measuring thermal conductivity and specific heat capacity values of inhomogeneous materials with a heat flow meter apparatus, Journal of Building Engineering, 9 (2017), 135-141, https://doi.org/10.1016/j.jobe.2016.11.011

[35] Carbonaro C, Cascone Y, Fantucci S, Serra V, Perino M, Dutto M. Energy Assessment of a PCM-Embedded Plaster: Embodied Energy Versus Operational Energy, Energy Procedia, 78 (2015), 3210-3215, http://dx.doi.org/10.1016/j.egypro.2015.11.782.

[36] Bianco L, Serra V, Vigna I, Energy assessment of a novel dynamic PCMs based solar shading: results from an experimental campaign, Energy and Buildings (2017), https://doi.org/10.1016/j.enbuild.2017.05.067.

[37] Komerska A, Bianco L, Serra V, Fantucci S, Rosiński M. Experimental Analysis of an External Dynamic Solar Shading Integrating PCMs: First Results, Energy Procedia, 78 (2015), 3452-3457, http://dx.doi.org/10.1016/j.egypro.2015.11.125.

[38] https://www.rubitherm.eu/en/productCategories.html <accessed 21.05.2017>

[39] Incropera F. P, DeWitt D. P. Fundamentals of Heat and Mass Transfer, 3rd ed. Wiley (1990).

[40] IBP, WUFI® 2D version 3, Fraunhofer Institute for Building Physics, Holzkirchen, Germany, https://wufi.de/en/software/wufi-2d/_ (14 May 2017).

[41] Künzel H M 1995. Simultaneous Heat and Moisture Transport in Building Components, Fraunhofer IRB Verlag Stuttgart, Germany. ISBN 3-8167-4103-7

[42] CEI ENV 13005:2000. Guide to the expression of uncertainty in measurement, (2000).

Appendix A

Table 4. Dataset. 2nd measurement cycle (24 – 48 h), more detailed experimental results (DHFM heat fluxes and temperatures with a more frequent time step of 666 seconds) are available at the following link: https://dl.dropboxusercontent.com/u/7103172/Dataset.xlsx

	PCM-a (paraffin wax)						PCM-b (salt-hydrate)					
	Test 1 (12 ºC amplitude sinusoidal solicitation)			Test 2 (6 ºC amplitude sinusoidal solicitation)			Test 1 (12 ºC amplitude sinusoidal solicitation)			Test 2 (6 ºC amplitude sinusoidal solicitation)		
time	$T_{PCM, core}$	$T_{PCM, up}$	$T_{PCM, low}$	$T_{PCM, core}$	$T_{PCM, up}$	$T_{PCM, low}$	$T_{PCM, core}$	$T_{PCM, up}$	$T_{PCM, low}$	$T_{PCM, core}$	$T_{PCM, up}$	$T_{PCM, low}$
s	ºC	ºC	ºC	ºC	ºC	ºC	ºC	ºC	ºC	ºC	ºC	ºC
0	26.0	26.2	26.4	26.4	26.5	26.6	24.2	24.4	24.4	24.3	24.4	24.5
1800	26.5	26.9	26.7	26.6	26.9	26.7	24.6	25.0	24.6	24.6	24.8	24.7
3600	26.9	27.5	27.0	26.8	27.2	26.8	25.0	25.6	25.0	24.8	25.1	24.9
5400	27.2	28.1	27.2	26.9	27.4	26.9	25.4	26.2	25.4	25.0	25.4	25.1
7200	27.4	28.5	27.3	27.1	27.7	27.0	25.7	26.7	25.6	25.3	25.7	25.3
9000	27.5	29.1	27.4	27.3	28.0	27.1	26.0	27.2	25.8	25.5	26.0	25.4
10800	27.7	29.8	27.5	27.4	28.2	27.2	26.2	27.8	26.0	25.7	26.2	25.5
12600	28.0	30.5	27.5	27.5	28.4	27.2	26.5	28.3	26.1	25.8	26.5	25.6
14400	28.6	31.3	27.6	27.6	28.6	27.3	27.0	29.0	26.8	25.9	26.6	25.7
16200	29.0	32.1	27.7	27.9	28.9	27.3	29.3	31.0	28.7	26.0	26.8	25.7
18000	29.6	32.8	27.8	28.1	29.2	27.3	30.3	31.9	29.6	26.0	26.9	25.8
19800	31.3	33.8	29.1	28.4	29.5	27.4	30.7	32.3	30.0	26.2	27.0	25.8
21600	33.0	35.3	30.9	28.6	29.6	27.4	31.0	32.4	30.1	26.4	27.2	26.0
23400	33.3	35.6	31.2	28.8	29.8	27.5	30.9	32.3	30.1	26.7	27.5	26.4
25200	33.3	35.5	31.2	28.9	29.9	27.5	30.7	32.1	29.9	27.3	28.0	26.9
27000	33.2	35.3	31.1	28.9	29.9	27.6	30.5	31.8	29.7	27.6	28.2	27.1
28800	32.9	34.9	31.0	29.0	29.9	27.6	30.2	31.4	29.5	27.8	28.3	27.3
30600	32.6	34.4	30.7	29.1	30.0	28.2	29.8	30.8	29.2	27.7	28.2	27.2
32400	32.1	33.7	30.5	29.3	30.0	28.5	29.3	30.1	28.7	27.5	27.9	27.1
34200	31.5	32.9	30.1	29.2	29.8	28.5	28.7	29.4	28.3	27.2	27.6	26.9
36000	30.9	32.1	29.7	29.0	29.4	28.3	28.1	28.6	27.8	26.9	27.3	26.7
37800	30.2	31.1	29.3	28.7	29.0	28.1	27.5	27.8	27.2	26.7	26.9	26.4
39600	29.6	30.2	28.8	28.2	28.5	27.9	26.8	26.9	26.6	26.3	26.5	26.1
41400	28.7	29.1	28.3	27.8	28.0	27.6	26.0	25.9	26.0	25.9	26.1	25.8
43200	27.9	28.0	27.8	27.3	27.4	27.3	25.3	25.0	25.4	25.5	25.6	25.5
45000	27.2	26.9	27.3	26.9	26.9	27.1	24.6	24.2	24.9	25.1	25.2	25.2
46800	27.7	27.3	27.7	27.5	27.3	27.5	24.0	23.3	24.3	24.7	24.7	24.9
48600	27.7	26.9	27.7	27.5	27.2	27.5	23.9	22.6	23.9	24.3	24.3	24.6
50400	27.7	26.4	27.7	27.4	27.0	27.5	24.1	23.0	24.5	23.9	23.8	24.3
52200	27.5	26.0	27.7	27.3	26.8	27.5	24.2	23.0	24.6	23.6	23.4	24.0
54000	27.2	25.5	27.7	27.2	26.6	27.6	24.2	22.9	24.7	23.7	23.3	23.9
55800	26.8	24.9	27.6	27.0	26.4	27.5	24.1	22.6	24.6	23.8	23.3	23.9
57600	26.4	24.3	27.5	26.8	26.2	27.5	23.9	22.3	24.5	24.0	23.3	24.0
59400	25.8	23.5	27.0	26.7	26.0	27.5	23.6	22.0	24.1	23.9	23.2	24.1
61200	24.6	22.4	25.7	26.4	25.7	27.4	23.0	21.3	23.3	23.8	23.1	24.1
63000	22.6	20.7	24.1	26.2	25.5	27.4	22.0	20.5	22.5	23.5	23.1	24.1
64800	21.5	19.8	23.3	25.9	25.2	27.2	21.2	19.7	21.8	23.5	23.1	24.2
66600	21.2	19.5	23.1	25.6	24.9	26.9	20.6	19.2	21.3	23.4	23.1	24.2
68400	21.2	19.6	23.1	25.3	24.6	26.4	20.3	19.0	21.0	23.4	23.1	24.2
70200	21.4	19.9	23.2	24.9	24.3	25.9	20.4	19.1	21.0	23.4	23.1	24.2
72000	21.7	20.2	23.4	24.6	24.1	25.6	20.5	19.4	21.1	23.4	23.1	24.2
73800	22.0	20.7	23.6	24.5	24.1	25.5	20.8	19.9	21.4	23.4	23.2	24.2
75600	22.5	21.3	23.9	24.7	24.3	25.5	21.2	20.4	21.8	23.4	23.2	24.1
77400	22.9	22.0	24.3	24.9	24.6	25.6	21.7	21.0	22.2	23.4	23.2	23.9
79200	23.5	22.7	24.7	25.1	24.9	25.8	22.3	21.8	22.7	23.4	23.3	23.9
81000	24.2	23.5	25.1	25.4	25.3	26.0	22.8	22.5	23.1	23.5	23.4	23.9
82800	24.8	24.4	25.5	25.7	25.7	26.2	23.2	23.1	23.5	23.7	23.7	24.0
84600	25.3	25.1	25.9	26.0	26.0	26.3	23.5	23.6	23.9	23.8	23.9	24.2

APPENDIX “B” (Paper draft)

Modeling and empirical validation of an algorithm for simulations of hysteresis effects in Phase Change Materials for building components.

Modeling and empirical validation of an algorithm for simulations of hysteresis effects in Phase Change Materials for building components.

Francesco Goia[a,1], Gaurav Chaudhary[b], Stefano Fantucci[c]

[a] *Department of Architecture and Technology, Faculty of Architecture and Fine Art, NTNU, Norwegian University of Science and Technology, Trondheim (Norway).*

[b] *The Research Centre on Zero Emission Buildings, Faculty of Architecture and Fine Art, NTNU, Norwegian University of Science and Technology, Trondheim (Norway).*

[c] *Department of Energy, Politecnico di Torino, Torino, Italy.*

Abstract

The use of Phase Change Materials (PCM) in different building applications is a hot topic in today's R&D activities. Numerical simulations of PCM-based components are often used both as a research activity and design tool, though present-day codes for building performance simulation (BPS) present some shortcomings that limit their reliability. One of these limitations is the impossibility to replicate effects given by thermal hysteresis – a characteristic of several PCMs.

In this paper, an original algorithm that allows hysteresis effects to be accounted for is described and compared against experimental data and data from other simulation environments. The algorithm is implemented in EnergyPlus™ and makes use of the Energy Management System (EMS) group, one of the high-level control methods available in EnergyPlus™. The algorithm enables the replication of PCM's different heating/cooling enthalpy curves in this BPS tool, where effects of thermal hysteresis cannot be so far simulated.

A comparison between numerical results and experimental data is provided, and it is possible to see the impact of the algorithm in the simulation of heat transfer in an opaque sandwich wall containing a layer made of PCM. A local sensitivity analysis complements this study.

[1] Postal address: Alfred Getz' vei 3, NO-7491 Trondheim, Norway; e-mail address: francesco.goia@ntnu.no, francegoia@gmail.com; tel.: +47 73 550 275; fax: +47 73 595 094.

Highlights

- Implementation of an algorithm for simulation of thermal hysteresis in PCM for *EnergyPlus*™.
- Verification of the algorithm through comparison with experimental data.
- Simulation of the effect of PCM hysteresis in opaque walls with a PCM layer.

Keywords

Building Simulation
Energy Management System (EMS)
EnergyPlus
PCM Hysteresis
PCM Modeling
Phase Change Materials (PCM)

Acronyms

BPS	Building Performance Simulation
DSC	Differential Scanning Calorimetry
EMS	Energy Management System
Erl	EnergyPlus Runtime Language
HVAC	Heating, ventilation, and air conditioning
BCVTB	Building Controls Virtual Test Bed
RT 28 HC	Paraffin wax based PCM with melting area around 28°C
SP 26 E	Salt hydrate based PCM with melting area around 26 °C
PCMH	Phase Change Material- Heating
PCMC	Phase Change Material- Cooling
PC	Poly-Carbonate
DHFMA	Dynamic Heat Flow Meter Apparatus
IC	Influence Coefficient
FVM	Finite Volume Method
FDM	Finite Difference Method

Nomenclature

$\|\Delta\|$	Absolute value of temperature difference	[°C]
E	Experimental temperature value	[°C]
PRMSE	Percentage root mean square error	[%]
RMSE	Root mean square error	[°C]
S	Numerical (simulated) temperature value	[°C]

EMS code nomenclature

Avg_Temp	EMS Global Variable
C_Wall	EMS Construction Index Variable for Plate Wall_C
Current_Wall	EMS Global Variable
Current_Wall_Status	EMS Output Variable for "Current_Wall"
EMS PCM Code	EMS Program
H_Wall	EMS Construction Index Variable for Plate Wall_H
Hysteresis	EMS Program Calling Manager
Node N	Calculation node inside the PCM layer
Node_PCM	EMS Sensor
PCM_Temp_Trend	EMS Trend Variable to record data of "Node_PCM"
Plate Wall_C	Construction with PCM which has cooling enthalpy-temperature curve
Plate Wall_H	Construction with PCM which has heating enthalpy-temperature curve
Wall	EMS Actuator
Wall_PCM	Name of Surface (wall) having PCM

1. Introduction

The interest in the adoption of phase change materials (PCMs) in several building applications, ranging from building components to HVAC systems, is steadily increasing over the last years in the R&D community. When integrated into building components such as walls, floors, partition walls, glazing systems, these materials have the potential to enhance the heat storage feature of the building fabric. This increased thermal capacity may determine a reduction and delay of the daily peak loads, with a consequent downsizing of the HVAC systems and increase of occupants' thermal comfort. It is out of the scope of this paper to review the innumerable research activities carried out in the last years on the use of PCM in buildings, and comprehensive recent overviews can be easily found in literature, both at technologies and systems level [1][2][3][4][5], and at materials level [6][7][8][9].

Several studies have shown important benefits related to thermal comfort, energy savings, and HVAC downsizing when these technologies are used in buildings. However, it must be noticed that much of these has been limited to laboratory scale testing, or small mock-up, while studies in real buildings have been rather limited. However, with advancement in numerical simulation tools, advantages given by the adoption of PCM in full-scale buildings can be studied through building performance simulation codes.

In the last decade, an explosion of studies based on numerical simulations of PCMs in buildings can be seen – in Figure. 1 the number of articles indexed in bibliographic database SCOPUS, which had Phase Change Materials, Simulation, and Building as a keyword or word used in their abstracts, is reported, for the period 2005-2015. Computer simulation tools provide a rapid and low-cost method to assess the performance of different systems, technologies, controls, and in general applications of PCM in full-scale buildings. Nonetheless, it is important to stress that to reach the expected/predicted performance; simulations should be done only when an accurate and validated model has been developed.

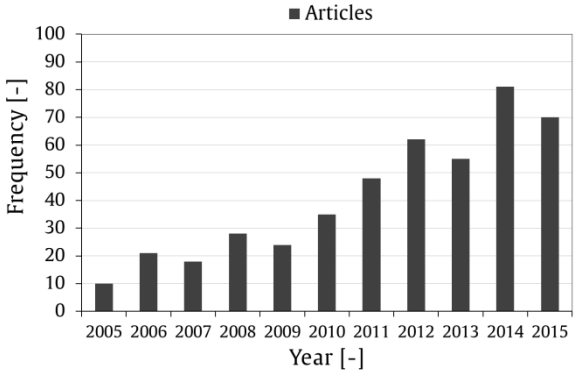

Figure 1. *Number of articles listed in the bibliographic database SCOPUS, which had Phase Change Materials, Simulation, and Building as a keyword or word used in their abstracts, is reported, for the period 2005-2015.*

Nowadays many detailed building simulation programs are available to assist engineers, architects, designers, researchers, and manufacturing companies to implement PCMs technologies and to evaluate innovative solutions capable of improving the energy and thermal performance of buildings. Most of these tools are listed by the U.S.

Department of Energy (DOE) web directory [10], and some of them implement modules for the solution of heat transfer and heat storage within PCMs, among which it is possible to list EnergyPlus, TRNSYS, ESP-r, WUFI Plus and BSim.

One intrinsic limitation of most of the PCM models which are integrated into a whole building simulation programs is the need to run simulations with a very small time step (i.e., in order of minutes) to achieve an acceptable level of accuracy. Because of this condition, a one-year thermal performance simulation becomes computationally heavy as iterative methods are used in each time step. Also, the convergence may not be achieved due to numerical instability especially when PCM enters or leaves the phase change region [11]. Currently, none of the whole building simulation programs are using efficient mathematical models that are quick, accurate and numerically stable at realistic time step.

Aside from this limitation, there are few more shortcomings that affect the full reliability of simulations of PCM in buildings. As highlighted in the literature [12][13][14], sub-cooling and thermal hystereses are two features recurring in many PCM that are not currently tackled by any BPS tools. The lack of algorithms and strategies to correctly simulate these aspects of the complex dynamic of PCMs can lead to wrong assumptions in designs as well as to not fully reliable findings in research and development.

Currently, there is no BPS tool that is capable of addressing thermal hysteresis effect of PCMs, since all the available platforms that allow the simulation of PCM-based components offers to the modeller the possibility to define just one enthalpy vs. temperature curve as a material property. This approach is in opposition to what experimentally verified for most of the PCMs, which always show, even with different extent depending on the nature of the PCM and on the speed of the melting/solidification process, two different peak transition temperature values, one for the melting process and one for the solidification process respectively.

1.1. Research aims

The aims of the research activities presented in this paper are:

- To empirically validate the performance of two simulation codes (*EnergyPlus*™, Wufi®Pro/Plus) in simulating building components implementing PCMs;
- To develop and validate of an algorithm that implements the hysteresis effect of PCMs by means of Energy Management System (EMS) in EnergyPlus.

The approach presented in this paper is suitable to take into consideration thermal hysteresis effect and sub-cooling effect since both can be addressed if different enthalpy vs. temperature curve can be used by the simulation tool. However, because of the lack of experimental data on sub-cooling phenomena, the verification of the proposed algorithm is only carried out for the case of hysteresis – hence the reason to limit to this field the title of the paper.

1.2. Background on PCM modelling

1.2.1. Energy Plus

Among all the possible BPS tools, the paper presents a strategy and an algorithm that can be directly implemented in *EnergyPlus*™. This software is one of the leading BPS tools and has been developed with financial support of the U.S. Department of Energy. Aside from several features that make this software very powerful for building simulation, it is also worth mentioning that it is freeware and it can thus be used without limitations for both research and professional purpose.

The capability of modelling PCMs was added to *EnergyPlus*™ program version 2.0, released in April 2007, by adding a conduction finite difference (object "*CondFD*") solution algorithm [15]. This algorithm uses a semi-implicit finite difference scheme based on the heat capacity method with an auxiliary enthalpy vs. temperature dataset to account for latent heat evolution [16]. Successful validations of this algorithm in combination with PCM modelling for previous versions of *EnergyPlus*™ were reported by Zhuang [17], Campbell [18], and Chan [19].

A custom version of EnergyPlus version 8.1 with new hysteresis model was developed in part with OSU and NRGSIM inc. The PCM hysteresis modelling methodology used in this custom version has not yet been implemented in the official release of EnergyPlus. It uses an equation based approach for modelling dynamic phase change materials "PCM's" with minimal inputs. The inputs are designed to match the results of differential scanning calorimeter "DSC" testing. The model uses polynomial fitting curves to describe the properties of PCM adapted from the Ginzburg-Landau theory of phase transitions [20]. It uses two hysteresis modelling methods, curve switch and curve track. The former method is used for partial phase transition whereas the latter is used for complete phase transition.

1.2.2. Wufi®Pro/Plus

WUFI® Pro [21] is a 1D hygrothermal heat and moisture simulation software developed by Fraunhofer IBP, Holzkirken, Germany [22]. The software was chose for the following test because it represent a very popular tool that allow to simulate transient coupled heat and moisture transfer phenomena in wall assemblies solving the system of equations of heat and moisture transport by using the Finite Volume Method (FVM). The calculation method of WUFI® Pro is based on the spatial discretization of the transport equations and uses the fully implicit scheme for the time discretization.

More recently WUFI® Plus based on coupling hygrothermal and energetic building simulation was developed by Fraunhofer IBP [23]. In the software, the resulting heat and mass fluxes solved at the building component surfaces are incorporated into zonal models.

Building components containing PCM can be simulated from WUFI® Pro 5.0 version and in WUFI® Plus [24] by assigning a temperature dependent enthalpy data in the hygrothermal function menu of the material/layer data editor.
Two main limitations of the software are reported in the literature: the first limitation is represented by the possibility to assign as input data only hourly weather profiles [24], and secondly, the impossibility to implement hysteresis effect

2. Numerical model

As discussed in the introduction, current BPS tools are unable to model thermal hysteresis effects in PCM due to the limitation that only one enthalpy-temperature curve can be provided as a material property. In this section, the modelling approach adopted to overcome this current limitation in EnergyPlus™ is presented, together with the explanation of the algorithm and its implementation in the simulation tool.

2.1. The EMS approach

The current version of EnergyPlus™ allows the modelling of a PCM layer to be carried out through the object "*MaterialProperty:PhaseChange*". This object is used to define the enthalpy vs. temperature curve of a given material, whose other thermophysical properties are defined in the object "*Material*", under the same group "*Surface Construction Elements*". A maximum of sixteen pairs of enthalpy-temperature values can be given to describe the non-linear dependence of the internal energy of a PCM on the temperature. The enthalpy correspondent to each temperature

point is independent from the direction of the energy storing process – i.e. if the material is cooling or heating. This means, in practice, that only one enthalpy vs. temperature curve can be defined, and it is, therefore, a common practice to provide the values of a "fictitious" curve, calculated as the average between the heating and the cooling enthalpy vs. temperature curves provided in the PCM datasheet. It is important to mention that the simulation of PCM can be only carried out using the algorithm "*ConductionFiniteDifference*" for the solution of the heat balance within the construction element.

Given the present-day fields of the object "*MaterialProperty:PhaseChange*", the strategy to overcome this limitation makes use of the group "*Energy Management System*" (EMS) and its objects [26]. EMS is an advanced feature of *EnergyPlus*™, and it is designed for users to develop customized high-level, supervisory control routines to override selected aspects of *EnergyPlus*™ modelling [27]. Conventional use of EMS in simulations are advanced HVAC modelling and controls[29][30][31], including faulty HVAC models for Fault Diagnostic Detection [28], real-time building energy simulation [29], co-simulation of several other building energy software codes with Energy Plus using Building Controls Virtual Test Bed (BCVTB) [30][31]. In addition, EMS has also been used as a tool to model occupant behavior in connection to adaptive comfort theory and occupancy control [32], or other advanced modelling of user's interaction, such as the stochastic use of windows [33]. Furthermore, EMS has also been used for simulation of behaviour and advanced control of dynamic properties in real [34][35] and ideal dynamic window systems [36].

EMS has nonetheless some limitations, and its use requires advanced knowledge of *EnergyPlus*™ and basic computer programming. A simple programming language called EnergyPlus Runtime Language (Erl) is used to describe the control algorithms, which are executed by the *EnergyPlus*™ engine when the simulation is carried out.

In the algorithm to enable the simulation of hysteresis effect of PCM, objects and programs of EMS are used to:

- *Step 1)* Evaluate the state of the heat storage process of the PCM layer at the simulation time-step (whether the PCM layer is cooling down or heating up compared to the previous time-step of the simulation);
- *Step 2)* Select the appropriate enthalpy vs. temperature curve, coherent with the direction of the heat storage process;
- *Step 3)* Instruct *EnergyPlus*™ to carry out the simulation of the time-step with the appropriate construction characterized by the "correct" enthalpy vs. temperature curve, depending on the direction of the heat storage process.

The evaluation of the heat storage process (Step 1), can be easily done through the EMS since the temperature of the internal nodes of a construction element are calculated by "*ConductionFiniteDifference*" algorithm and can be directly acquired by the EMS. A simple way to assess the direction of the heat storage process within the PCM layer is to compare the temperature of a node inside the PCM layer, at the time-step, with the temperature of the same node at the previous time-step: if it is greater, the layer is increasing its internal energy, and a heating (melting) process is taking place; if it is lower than that at the previous time-step, the layer is cooling down (solidifying).

For the execution of Step 2, the EMS selects among two different objects "*Construction*", previously defined by the modeller, the first one related to a wall structure implementing a PCM with an enthalpy vs. temperature curve for heating process and the second one related to a wall structure implementing a PCM with an enthalpy vs. temperature curve for cooling process.

The EMS program is then used, in Step 3, to instruct *EnergyPlus*™ to carry out the simulation with the right "*Construction*" object, previously selected based on the heating or cooling process (Step 1).

2.2. Preliminary settings

Before defining the right program in the EMS environment, it is necessary to set an appropriate space discretization for the numerical solution of the heat transfer equation. The space discretization must be so that at least one node falls inside the PCM layer. This node (named **Node N** in these sections) will be recalled in the EMS program. Space discretization is controlled in EnergyPlus™ through a parameter called "*Space Discretization Constant*" in the object "*HeatBalanceSettings:ConductionFiniteDifference*".

Furthermore, the values used to define the enthalpy vs. temperature curve cannot be directly changed by the EMS, but belong to a specific object in the category "*MaterialProperty:PhaseChange*", it is necessary to define, for each PCM, two objects "*MaterialProperty:PhaseChange*" – one implementing the enthalpy vs. temperature curve for heating process, and one implementing the enthalpy vs. temperature curve for cooling process. Moreover, each object "*MaterialProperty:PhaseChange*" needs to be connected to a main object "*Material*", where the other thermophysical and optical properties of a construction material are given, two objects "*Material*" need to be defined – one for the PCM during the heating process and one for the PCM during the cooling process. If the PCM is not the only layer of a construction element (as usually happens), it is then necessary to define two different "*Construction"* objects, where the two different "*Material*" objects are coupled with other layers to form the construction element. For the sake of this explanation, the two "Constructions" objects are called **Plate Wall_H** (corresponding to the PCM with the enthalpy vs. temperature curve for the heating process), and **Plate Wall_C** (corresponding to the PCM with the enthalpy vs. temperature curve for the cooling process).

Once these two pre-settings are implemented, it is possible to move to the EMS group and define the objects and program necessary to execute the simulation.

2.3. Working algorithm code

The EMS objects and how they can be used in *EnergyPlus*™ to make the algorithm for the hysteresis modelling have discussed in detail in ***Appendix A***.

3. Validation

The performance of EnergyPlus and WUFI PCM module was compared with the experimental data without considering Hysteresis effect. Furthermore, the performance of the EMS code described in the above section was verified against experimental data from measurements in a Dynamic Heat Flow Meter Apparatus (DHFMA). The aim of this section is to show the impact of the EMS code on the simulation of the PCM's layer temperature evolution and to highlight that the proposed approach allows a better agreement between experimental data and numerical simulations to be achieved.

3.1. The GHFM experimental analysis

Laboratory measurements were performed by means of DHFMA [24][37], evaluating the response of PCM under sinusoidal periodic solicitations as reported in [38][39]. Tests were performed by using two different solicitations, aimed at on one hand to reach a complete phase transitions (Test 1) and on the other hand to reach only a partial phase transition (Test 2).

220 **3.1.1. Specimens**

221 For this study, two different types of PCMs were used, one characterized by a moderate thermal hysteresis (PCM-
222 a) and one characterized by a much more relevant thermal hysteresis (PCM-b).

223 The first PCM-a is a paraffin-based PCM product named "RT 28 HC" by RUBITHERM GmbH [40]. The thermal
224 properties of this PCM, derived from the technical data sheet, are given in Table 1. Data to calculate the specific heat
225 vs. temperature and the enthalpy vs. temperature curves were also obtained from the technical datasheet.

226 The second PCM-b is a salt hydrate product named "SP 26 E" by RUBITHERM GmbH **Errore. L'origine**
227 **riferimento non è stata trovata.**, whose thermo physical properties are reported in Table 1. This type of PCM usually
228 shows much higher energy storage density (i.e. narrower melting/congealing range) than paraffin-based PCM.
229 Hysteresis effects in salt hydrates are also more relevant than in paraffin because of the combination of the
230 thermophysical properties of these materials (higher thermal conductivity, higher density, higher energy storage
231 density). This characteristic can be well understood comparing the enthalpy vs. temperature curves of the PCM–a (Fig.
232 2) with those of the PCM–b (Fig. 3). The area between the curve for the heating process and the one for the cooling
233 process gives the impact of the hysteresis effect: the larger the area, the higher the effect on the thermal behavior of the
234 PCM due to the hysteresis. This area is at least 10 times larger in Fig. 3.b (PCM-b) than in Fig. 2.b (PCM-a).

Table 1. Thermophysical properties of the two PCMs.

Name	**Material Class**	**Melting range**	**Congealing range**	**Specific heat capacity**	**Density (solid)**	**Density (liquid)**	**Conductivity**
		[°C]	[°C]	[kJ/kg·K]	[kg/l]	[kg/l]	[W/(m·K)]
PCM-a	Paraffin Wax	27-29	29-27	2.0	0.88	0.77	0.2 (both phases)
PCM-b	Salt Hydrate	25-27	25-24	2.0	1.50	1.40	0.6 (both phases)

235

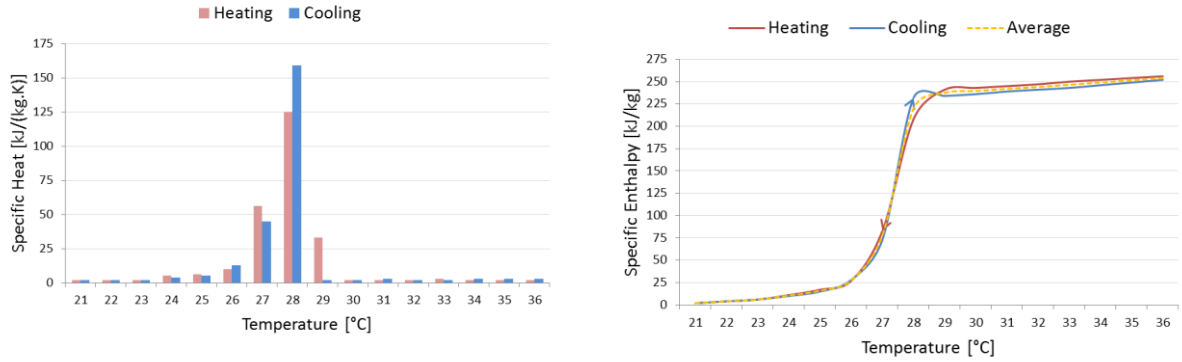

(a) **(b)**

Figure 2. Specific heat vs. temperature (a) and enthalpy vs. temperature (b) for heating and cooling process of the PCM-a (paraffin wax)

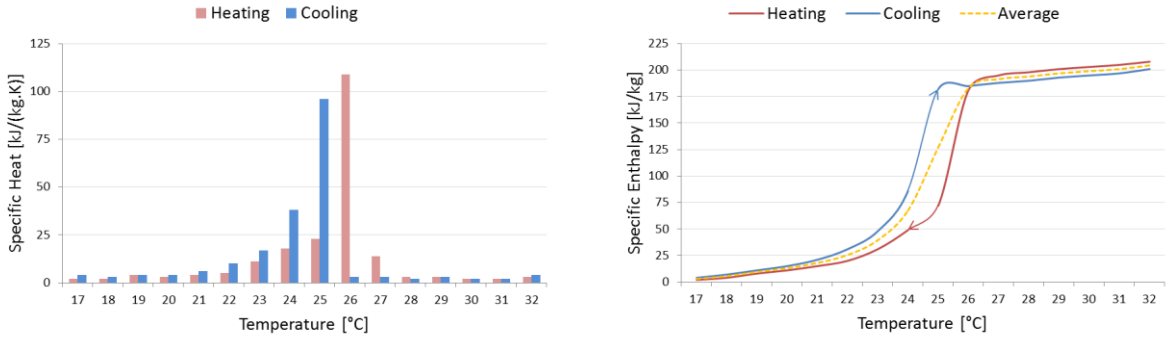

(a) **(b)**

Figure 3. Specific heat vs. temperature (a) and enthalpy vs. temperature (b) for heating and cooling process of the PCM-b (salt hydrate)

The two PCMs were choosen for their easy availability and because of their wide diffusion for the use in buildings. Nevertheless, another important criterion for the selection of the two PCMs is the different hysteresis behaviour related to their composition.

The two PCM specimens was built by filling a hollow polycarbonate panel 10 mm thick; thess methods were already tested in [42][43] and represent a fast and easy way to enclose PCM in a stabilized shape that allow to perform measurements by using a DHFM apparatus.

The polycarbonate panel filled with PCM were sandwiched between two gypsum board panels (thickness 12.5 mm) in order to avoid the direct contact between the PCM filled polycarbonate and the instrument plates, this solution allow to measure the temperature in the upper and lower interface of PCM neglecting the influence of the GHFM plates that are both at controlled temperatures.

The physical characteristics of each layer are illustrated in Table 2. Moreover the enthalpy/temperature curves of the two PCM are illustrated in Figure 2 & 3.

Table 2. Physical properties of each material that constitute the specimen. * (Average value between solid and liquid phase).

`	Name	d	ρ	c	λ
		[mm]	[kg/m^3]	[J/kg/K]	[W/mK]

1	Gypsum board	12.5	720	1090	0.19
2	Poly-carbonate	0.5	1200	1200	0.20
3	PCM-a	9.0	825*	2000	0.20
	PCM-b		1450*	2000	0.6
4	Poly-carbonate	0.5	1200	1200	0.20
5	Gypsum board	12.5	720	1090	0.19

250

251 **3.1.2. Experimental setup**

252 Experimental test were carried out by means of a Lasercomp FOX600 single sample guarded heat flow meter
253 apparatus. Temperatures were measured by means of type-E thermocouples (measurement accuracy ±0.25 °C),
254 connected to an external data logger. Thermocouples were placed in the PCM core, and at the upper and lower
255 boundaries of the polycarbonate PCM filled panel.

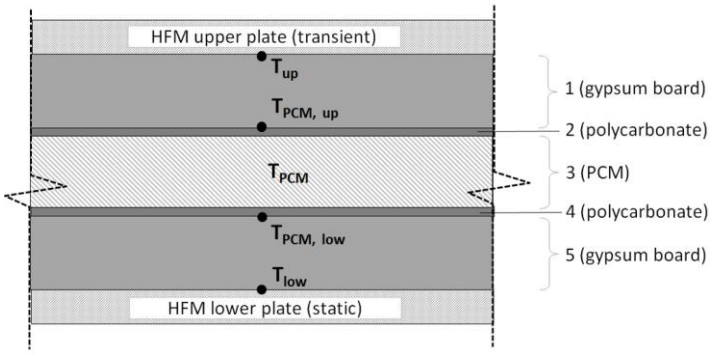

256

257 Figure 4. Layout of the measured specimen

258 The Heat Flow Meter Apparatus generally used for steady state thermal conductivity measurement was adjusted to
259 perform dynamic experiments imposing a sinusoidal temperature solicitation (periodic cycle of 24 h) in the upper plate
260 and maintaining at constant temperature the lower plate. The experiments were considered concluded after two
261 sinusoidal cycle (test duration = 48 h). Nevertheless, the first 24 h cycle were used only as initialisation period and were
262 afterwards discarded, in this way only the last 24 h cycle was considered for further analysis. As mentioned the test
263 were carried out on the two PCM imposing a lower plate temperature equal to the nominal melting temperature of the
264 PCM, and an upper temperature solicitation with different amplitudes, respectively of ±12°C for testing the complete
265 phase transition (Test 1) and ±6 °C to test partial phase transition (Test 2). The test conditions are summarised in Table
266 3.

Table 3. Test conditions

Specimen	Test condition	Upper plate temperature [°C]	Amplitude [°C]	Lower plate temperature [°C]
PCM-a	Test 1	16 - 40	±12	28

	Test 2	22 - 34	±6	28
PCM-b	Test 1	14 - 28	±12	26
	Test 2	20 - 32	±6	26

3.2. Validation method: Simulation of a virtual heat flux meter apparatus in BES software

The heat flux meter apparatus experiments were done virtually using both and EnergyPlus™ v. 8.4 and WUFI® Pro. The temperature values of upper plate (sinusoidal) and lower plate (constant) were forced as surface temperature of the wall imposing a surface convection coefficient h_c infinitely high. The settings of the simulation were arranged as it follows. In EnergyPlus™ the heat balance algorithm was set to Conduction Finite Difference Method, and Crank Nicholson Second Order "Difference Scheme" was used for calculations. "*Space Discretization Constant*" was set to 0.5 whereas "*Relaxation Factor*" was set to 0.01. "*Inside Face Surface Temperature Convergence Criteria*" was set to the minimum possible value, i.e. 10^{-7}.

Simulations were carried out using the same boundary conditions imposed in the experiments. Simulation runs were long enough so that a periodically stabilized response was achieved. Four runs were carried out to test the effect of the algorithm for hysteresis with different features of the PCM layer:

- EP_COOL: the wall sample was simulated using the conventional approach in EnergyPlus™ and using as the only enthalpy vs. temperature curve the curve related to the cooling process in Fig. 3;
- EP_HEAT: the wall sample was simulated using the conventional approach in EnergyPlus™ and using as the only enthalpy vs. temperature curve the curve related to the heating process in Fig. 3;
- EP_AVG: the wall sample was simulated using the conventional approach in EnergyPlus™ and using as the only enthalpy vs. temperature curve the fictitious curve obtained as the average of the heating and cooling curves, shown in Fig. 3;
- EP_EMS (only in *EnergyPlus*™): the wall sample was simulated using the EMS approach presented in this paper to account for thermal hysteresis effects (and thus with both the two enthalpy vs. temperature curves for heating and cooling process illustrated in Fig. 3).

Computational times for the three simulations were identical, considering possible small changes due to a different use of the CPU. It is possible to affirm that the use of the EMS (in the algorithm for the simulation of hysteresis effects, EP_HYS) does not increase the computational load of the simulation, and thus does not have any drawback from a functional point of view.

Additionally, three simulation runs (WUFI_HEAT, WUFI_COOL, and WUFI_AVG) were also carried out on WUFI® Pro v. 6.1. The settings of the simulation were arranged as it follows. In *WUFI® Pro* (based on the finite volume method), space was discretized by using the option coarse grid (100 elements) with adaptive mesh refinement at the boundary of each layer, while the time discretization was equal to the DHFM measurement output (666 seconds). Moreover, in the numeric window, the options *increased accuracy* and *adapted convergence* where flagged, while the *moisture transport calculation* was excluded.

A custom version of Energy Plus developed by NRGSIM was also tested for all the 4 cases. Test 1 for both PCMs where complete phase transition is seen, Curve Track options was selected for the hysteresis modelling methodology whereas for Test 2 of for both PCMs where incomplete phase change happens, Curve Shift is used. In the graphs shown in later sections and Appendix B, the simulation result from this model is shown with name "NRGSIM".

3.3. Results

Experimental data and numerical data from the four rounds of simulation (EP_COOL, EP_HEAT, EP_AVG and EP_HYS) were compared both quantitatively and qualitatively. Values of internal temperature nodes were used to carry out the verification of the modelling approach and to assess its performance.

Quantitative estimation of the matching between numerical and experimental results was carried out through the use of the following indices:

- Percentage root mean square error (PRMSE, [%]), calculated according to the Eq. (1) :

$$PRMSE = \sqrt{\frac{1}{n} \cdot \sum_{j=1}^{n} \left(\frac{s_j - e_j}{e_j}\right)^2} \quad (1)$$

  ,where n is the total number of readings over a certain period, and e_j and s_j are the experimental and simulated values, respectively.

- Root mean square error (RMSE [°C]), calculated according to the Eq. (2):

$$RMSE = \sqrt{\frac{1}{n} \cdot \sum_{j=1}^{n} (s_j - e_j)^2} \quad (2)$$

- The average value of the absolute difference between simulated and measured values $|\Delta|$ [°C] Eq.(3) :

$$|\Delta| = \frac{1}{n} \cdot \sum_{j=1}^{n} |s_j - e_j| \quad (3)$$

In Table 4 the values of PRMSE, RMSE and |Δ| for the four PCMs for the four different runs are reported. These error values are with simulation done on EnergyPlus™ Version 8.4.

Table 4. *Thermophysical properties of materials constituting the wall sample layers.*

Method	PCM	PRMSE [%]	RMSE [°C]	|Δ| [°C]
EMS	RT28_6	3.7%	0.99	0.80
	RT28_12	4.0%	1.05	0.69
	SP26_6	3.2%	0.78	0.70
	SP26_12	4.3%	0.99	0.82
AVG	RT28_6	4.1%	1.09	0.90
	RT28_12	4.5%	1.20	0.80
	SP26_6	4.8%	1.20	1.01
	SP26_12	4.4%	1.07	0.96
COOL	RT28_6	4.1%	1.10	0.90
	RT28_12	4.7%	1.28	0.81
	SP26_6	5.0%	1.27	1.04
	SP26_12	4.9%	1.20	1.05
HEAT	RT28_6	4.1%	1.08	0.90
	RT28_12	11.1%	2.59	1.98
	SP26_6	5.0%	1.20	1.03
	SP26_12	4.0%	1.00	0.85

Qualitative verification was carried out comparing the time profiles for stabilized period of the simulated and experimental temperature values. The temperature evolution inside the PCM layer of each wall sample is shown in Fig. 5 and in Fig. 6 for the wall with the PCM-a "SP 26 E" and the wall with the PCM-b "RT 28 HC", respectively. Fig 5 and 6 shows the experimental data with EP_EMS and NRGSIM model simulation data with EP_AVG and WUFI_AVG where average of heating and cooling curves is used. Individual graphs of each individual software with experimental and EP_EMS is shown in Appendix B.

Results highlight that both EnergyPlus and WUFI are sufficiently accurate only to simulate PCM characterised by low hysteresis during their complete phase transitions, the main differences among the results of the two software are due to lack of accurate synchronisation in WUFI, in fact as highlighted in [24] one of the limitation of the lath software is that only hourly time profile interpolated for smaller time steps can be assigned as boundary condition.

The comparison between the output of the simulations and the experimental data demonstrates the reliability of the proposed approach for the simulation of PCM-based components in EnergyPlus™ Version 8.4. Quantitatively, a slightly better match (lower PRMSE and RMSE) between experimental data and simulation is recorded when the new algorithm, i.e. EP_EMS is adopted compared to other approaches. Furthermore using the EMS_EP, higher improvement in the results was seen in incomplete melting conditions (tests 2).

Qualitatively, the effect of the algorithm accounting for the hysteresis effects is identifiable in Figure 7. There, it is possible to see that by using EP_EMS both during the heating and cooling process the obtained numerical solution from the algorithm are closer to experimental data if compared to the other simulation methods that does not account hysteresis, as expected this is particularly important for the salt hydrate PCM-a. When the comparison is carried out with the numerical simulation that made use of the averaged enthalpy vs. temperature curve (SIM_AVG), the difference between the simulation with the proposed method and the conventional approach is less evident, yet still present.

The simulation results of NRGSIM model compared with experimental and EP_EMS simulation results can be seen in Appendix B. While this approach obtained closer numerical solution while cooling, it obtained significant error in heating phase. Somehow after using both available methods of PCM hysteresis modelling strategies, none of them gives acceptable results when compared to experimental data. Whereas in usability terms, the major flaw in using this version is that the while official version of EP uses Enthalpy-Temperature curve data to model PCM, this NRGSIM model uses polynomial fitting curves to describe the properties of PCM. This poses a challenge to modellers as by using polynomial fitting curves method, they might not be able to represent Enthalpy-Temperature curve accurately which may further lead to inaccuracies in the result.

The scope of this verification was to demonstrate the functioning of the proposed algorithm (EP_EMS) and to show that the changes in the numerical solution were coherent with the expected behaviour.

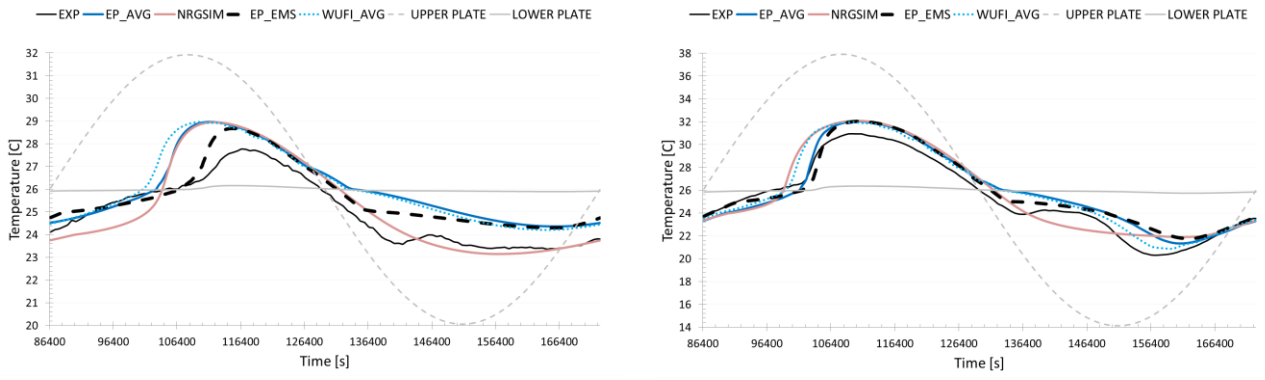

(a) **(b)**

Figure 5. *Temperature evolution of SP26E under a stabilized periodic cycle. (a) Comparison between experimental data and simulations with sinusoidal amplitude of ±6; (b) Comparison between experimental data and simulations with sinusoidal amplitude of ±12.*

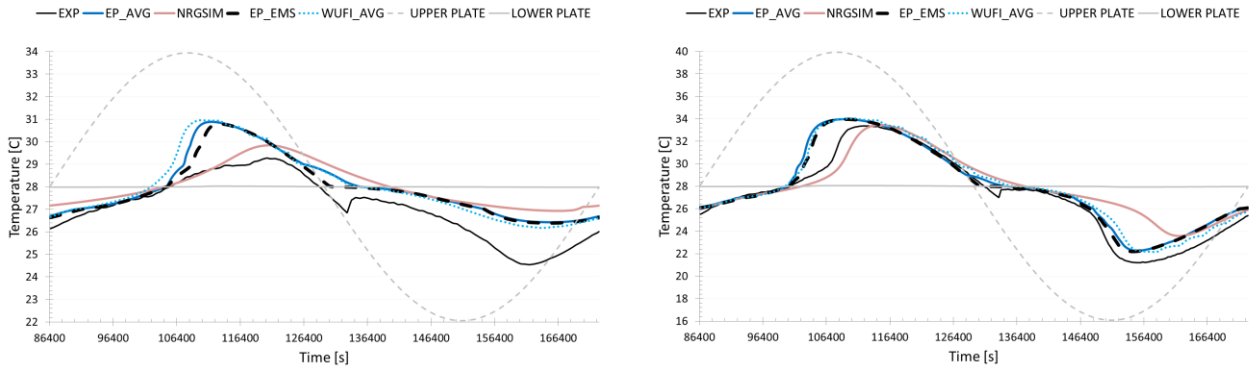

(a) **(b)**

Figure 6. *Temperature evolution of RT28HC under a stabilized periodic cycle. (a) Comparison between experimental data and simulations with sinusoidal amplitude of ±6; (b) Comparison between experimental data and simulations with sinusoidal amplitude of ±12.*

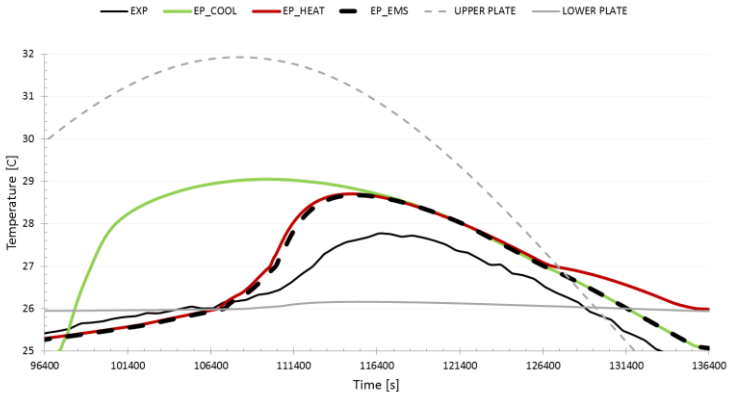

Figure 7. *Temperature evolution of SP26E under a stabilized periodic cycle. with a sinusoidal amplitude of ±6;*

Results on PCM-a demonstrate that both Energy Plus and WUFI can be used for PCM characterised by low hysteresis (PCM-a). Nevertheless, all the models are not totally accurate when were applied to simulate incomplete phase transition of the PCMs (tests 2).

4. Local Sensitivity Analysis

To highlight the parameters and inputs that are particularly influential (sensitive) to the final error difference between the simulation results and experimental results, a local sensitivity analysis was applied on the EP simulation model which uses the EMS algorithm discussed in the above sections. In particular, all the properties of the materials used in the wall specimen were used as the parameters for this sensitivity analysis.

4.1. Methodology

In the following sensitivity analysis, 14 parameters were chosen which represented the thermo-physical properties of the materials used in the specimens which were then applied a perturbation of ± 5% to their nominal value. The output of each simulation was |Δ| (degree) which is an average of the difference between the temperature of each time step of experimental and simulated values. The influence of each parameter is calculated from Equation (4) that represents the dimensionless "Influence Coefficient" (*IC*) [44], which is the percentage of changing in the output due to a percentage of perturbation in the input.

$$IC = \frac{\Delta OP \div \Delta OP_{BC}}{\Delta IP \div \Delta IP_{BC}} \quad (4)$$

Where ΔOP and ΔIP represents the changes in output and input, respectively; and ΔOP_{BC} and ΔIP_{BC} are the output and the input base case values.

4.2. Results & Discussion

The complete bar diagram of the "Influence Coefficient" for 14 analysed parameters is reported in Figure 8. From the results we can see that the most influential parameters on the algorithm are the density of PCM and the thickness and conductivity of Gypsum Board. These results can partially justify the difference among predicted and measured temperatures since the measurement uncertainty for each influential parameter are not well known, especially for data retrieved from literature (measurement uncertainty are not provided). This highlights that the measuring uncertainty of the highest sensitive parameters has to be carefully evaluated when experimental data is used to validate code.

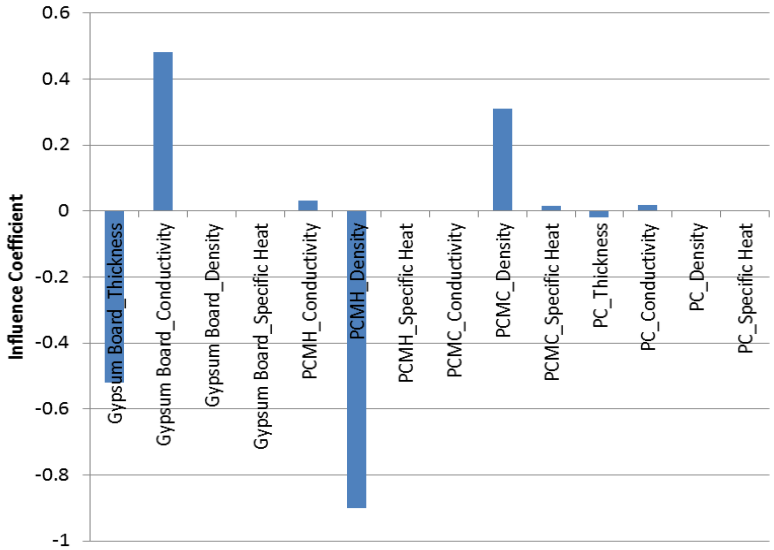

Figure 8. *Influence coefficient of selected 14 parameters*

5. Discussion

In the presented study, the reliability of two different building simulation software (Energy Plus and WUFI) were tested for the simulations of different type of bulk PCMs under different sinusoidal temperature conditions (complete and incomplete phase transition). Results reveal that both software are adequate to simulate PCM characterised by low

hysteresis during their complete phase transitions indicating not a significant mismatch in the temperature profile (synchronisation). On the contrary, high inaccuracies occur when they are used to simulate incomplete phase transitions and PCM characterised by significant hysteresis.

Moreover, a newly developed approach for the modelling of thermal hysteresis features in PCM has been developed and tested to prove that it is a robust and reliable algorithm that can be executed in *EnergyPlus*™ without increasing the computational load. Numerical results obtained through this method are coherent with the physical phenomena, and it has been shown that other, simplified simulation approaches that neglect hysteresis can lead to significant over-/under-estimation of the temperature evolution inside a wall that contains a PCM layer.

For this sake, a IDF file (an acronym for input data file, the compiled file that contains data to be processed by the *EnergyPlus*™ engine for simulation) for *EnergyPlus*™ Version 8.4 is attached to this paper as Supplementary material, and it can be used to replicate the simulations presented in Section 4. By changing the values of the enthalpy vs. temperature curves in the objects "*MaterialProperty:PhaseChange*" researchers can test different types of PCMs.

When it comes to the application of the presented modelling approach for design of wall systems and indoor climate control through the adoption of PCMs, the paper has shown that hysteresis effects for some PCMs can be very relevant to the extent that the temperature swing inside a PCM layer can be lower than for other PCMs that show little hysteresis. This characteristic can be beneficial for some applications of PCMs and analyses on the impact of hysteresis features on energy, and indoor environmental performance of the building is, therefore, an interesting topic, especially in combination with natural ventilation and free cooling – two strategies often used in combination with PCM systems.

So far, hysteresis has been mostly considered a drawback and conventional guidelines for the selection of PCM, at least for building applications which usually recommend avoiding materials showing high hysteresis. Dedicated research activities should instead be carried out to deepen this aspect and to unveil potential beneficial effects of thermal hysteresis.

6. Conclusions

The lack of suitable models to account the effect of thermal hysteresis of PCMs is nowadays a major shortcoming of BPS tools; well acknowledged in the scientific literature. In this paper, a new modelling approach, applicable to the latest versions of *EnergyPlus*™, which overcomes this limitation, is presented.

The novel algorithm makes use of the EMS group in *EnergyPlus*™ and allows the implementation of two "enthalpy vs. temperature" curves to correctly model both the melting and the congealing process of PCMs. The full set of code scripts for the EMS group is given in the paper so that it can be easily adopted by researchers and professionals that make use of this software for building performance simulation. Thought the modelling strategy presented in this paper is functioning for *EnergyPlus*™, the approach behind it can be replicated for other BPS tools using their own features and programming languages.

The verification of the code against experimental data demonstrated the reliability of the modelling approach and showed coherence between the achieved numerical results and the expected behavior of the code. Computational load due to the use of EMS is not increased compared to conventional modelling strategy in *EnergyPlus*™ that does not account for hysteresis effects. The presented algorithm is therefore robust, reliable, and computationally efficient (at least compared to other available codes).

The simple numerical study presented in Section 3 highlights how hysteresis effects can be very relevant for the temperature evolution inside a wall assembly; in the case, PCMs characterized with high hysteresis feature are adopted. In these cases, a conventional modelling approach that neglects thermal hysteresis may lead to substantially different

results, jeopardizing the outcomes of the simulation study. The numerical analysis described in the paper also suggests that hysteresis can represent a useful feature and that it can be used to achieve better energy and indoor environmental performance, is suitably tuned. This topic is definitely of high interest and, thanks to the novel algorithm presented in the paper, further research activities on the exploitation of hysteresis features can be carried out.

Moreover, the method described in this article is directly applicable to *EnergyPlus*™, but developers of other BPS tools can make use of this approach for the sake of other BPS codes and translate it to the correspondent program language for the implementation in different numerical tools.

7. Acknowledgments

This work has been supported by the Research Council of Norway and several partners through The Research Centre on Zero Emission Buildings (ZEB) at the Norwegian University of Science and Technology.

The authors want to express their gratitude to Alice Lorenzati, Rocco Costantino, and Maurizio Bressan for the helpful support during the experimental activities. Part of the research activities presented in this paper was carried out in the framework of a short term scientific mission supported by the European Union COST Action TU1403 (Adaptive Facades Network). The authors gratefully acknowledge the COST Action TU1403 for provided the excellent scientific network.

8. References

[1] M. Iten, S. Liu, A. Shukla, A review on the air-PCM-TES application for free cooling and heating in the buildings, Renew. Sustain. Energy Rev. 61 (2016) 175–186.

[2] A. Mavrigiannaki, E. Ampatzi, Latent heat storage in building elements: A systematic review on properties and contextual performance factors, Renew. Sustain. Energy Rev. 60 (2016) 852–866.

[3] E. Osterman, V. Butala, U. Stritih, PCM thermal storage system for “free” heating and cooling of buildings, Energy Build. 106 (2015) 125–133.

[4] N. Soares, J.J. Costa, A.R. Gaspar, P. Santos, Review of passive PCM latent heat thermal energy storage systems towards buildings’ energy efficiency, Energy Build. 59 (2013) 82–103. doi:10.1016/j.enbuild.2012.12.042.

[5] M. Pomianowski, P. Heiselberg, Y. Zhang, Review of thermal energy storage technologies based on PCM application in buildings, Energy Build. 67 (2013) 56–69. doi:10.1016/j.enbuild.2013.08.006.

[6] H. Akeiber, P. Nejat, M.Z.A. Majid, M.A. Wahid, F. Jomehzadeh, I. Zeynali Famileh, J.K. Calautit, B.R. Hughes, S.A. Zaki, A review on phase change material (PCM) for sustainable passive cooling in building envelopes, Renew. Sustain. Energy Rev. 60 (2016) 1470–1497. doi:10.1016/j.rser.2016.03.036.

[7] C.Y. Zhao, G.H. Zhang, Review on microencapsulated phase change materials (MEPCMs): Fabrication, characterization and applications, Renew. Sustain. Energy Rev. 15 (2011) 3813–3832. doi:10.1016/j.rser.2011.07.019.

[8] F. Souayfane, F. Fardoun, P. Biwole, Phase Change Materials (PCM) for cooling applications in buildings: A review, Energy Build. (2016).

[9] S. Kalnæs, B. Jelle, Phase change materials and products for building applications: a state-of-the-art review and future research opportunities, Energy Build. (2015).

[10] U.S.A. Department of Energy Building Energy Software Tools Directory, (n.d.). http://www.buildingenergysoftwaretools.com/.

[11] S.N. Al-Saadi, Z. Zhai, Modeling phase change materials embedded in building enclosure: A review, Renew. Sustain. Energy Rev. 21 (2013) 659–673. doi:10.1016/j.rser.2013.01.024.

[12] C.C.M.B. and C.B.N. P C Tabares-Velasco, Verification and Validation of EnergyPlus Conduction Finite Difference and Phase Change Material Models for Opaque Wall Assemblies, Build. Environ. (2012) 1–55. doi:10.1080/19401493.2011.595501.

[13] N. Brown, S. Philip, I.S. Trojaola, S. Ubbelohde, G. Loisos, CALIBRATION OF AN ENERGYPLUS SIMULATION OF A PHASE CHANGE MATERIAL PRODUCT USING EXPERIMENTAL TEST CELL DATA Loisos + Ubbelohde , Alameda , CA California College of the Arts , San Francisco , CA University of California , Berkeley , Berkeley , CA, (2014) 268–275.

[14] J. Kośny, PCM-Enhanced Building Components, Springer International Publishing, Cham, 2015. doi:10.1007/978-3-319-14286-9.

[15] U.S.A. Department of Energy New Features in Version 2.0.0, (n.d.).

[16] C.O. Pedersen, Advanced zone simulation in EnergyPlus: Incorporation of variable properties and phase change material (PCM) capability, Build. Simul. 2007. (2007) 1341–1345.

[17] C. Zhuang, A. Deng, Y. Chen, S. Li, H. Zhang, G. Fan, Validation of Veracity on Simulating the Indoor Temperature in PCM Light Weight Building by, Life Syst. Model. (2010) 486–496.

[18] K.R. Campbell, Phase change materials as a thermal storage device for passive houses, 2011.

[19] A. Chan, Energy and environmental performance of building façades integrated with phase change material in subtropical Hong Kong, Energy Build. 43 (2011) 2947–2955. doi:10.1016/j.enbuild.2011.07.021.

[20] https://github.com/nrgsim/EnergyPlus-Fortran/_<accessed 26 May 2017>

[21] IBP,WUFI® Pro, Fraunhofer Institute for Building Physics, Holzkirchen, Germany, https://wufi.de/en/software/wufi-pro/_<accessed 14 May 2017>.

[22] Künzel H M 1995. Simultaneous Heat and Moisture Transport in Building Components, Fraunhofer IRB Verlag Stuttgart, Germany. ISBN 3-8167-4103-7

[23] IBP,WUFI® Plus, Fraunhofer Institute for Building Physics, Holzkirchen, Germany, https://wufi.de/en/software/wufi-plus/_<accessed 14 May 2017>.

[24] Kosny, Jan, PCM-enahanced building components, An Application of Phase Change Materials in Building Envelopes and Internal Structures. Springer (2015). doi: 10.1007/978-3-319-14286-9.

[25] Baghban MH, Hovde PJ, Gustavsen A (2010) Numerical simulation of a building envelope with high performance materials. In: Proceedings of the 2010 COMSOL conference, Paris

[26] U.S. DOE, Application Guide for EMS: Energy Management System Used guide, US Dep. Energy. (2015). https://energyplus.net/sites/all/modules/custom/nrel_custom/pdfs/pdfs_v8.3.0/EMS_Application_Guide.pdf.

[27] P.G. Ellis, P.A. Torcellini, Simulation of energy management systems in EnergyPlus, in: Build. Simul. 2007, BS 2007; Beijing; China; 3-6 Sept. 2007, Beijing, 2007. http://www.nrel.gov/docs/fy08osti/41482.pdf.

[28] Mangesh Basarkar, X. Pang, L. Wang, P. Haves, T. Hong, Modeling and simulation of HVAC faults in EnergyPlus, IBPSA Build. Simul. (2013) 14–16.

[29] X. Pang, P. Bhattacharya, Z. O'Neill, P. Haves, M. Wetter, T. Bailey, Real-Time Building Energy Simulation Using Energyplus and the Building Controls Virtual Test Bed, in: Proc. Build. Simul. 2011 12th Conf. Int. Build. Perform. Simul. Assoc. Sydney, 14-16 Novemb., 2011: pp. 14–16.

[30] M. Wetter, Co-simulation of building energy and control systems with the Building Controls Virtual Test Bed, J. Build. Perform. Simul. 4 (2011) 185–203. doi:10.1080/19401493.2010.518631.

[31] X. Pang, M. Wetter, P. Bhattacharya, P. Haves, A framework for simulation-based real-time whole building performance assessment, Build. Environ. 54 (2012) 100–108. doi:10.1016/j.buildenv.2012.02.003.

[32] T. Hong, Occupant Behavior: impact on energy use of private offices, in: ASim 2012 - 1st Asia Conf. Int. Build. Perform. Simul. Assoc., 2012.

[33] S. Dutton, H. Zhang, Y. Zhai, E. Arens, Y.B. Smires, S. Brunswick, K. Konis, P. Haves, Application of a stochastic window use model in EnergyPlus, in: Proc. 5th Natl. Conf. IBPSA-USA, 2012.

[34] F. Favoino, F. Fiorito, A. Cannavale, G. Ranzi, M. Overend, Optimal control and performance of photovoltachromic switchable glazing for building integration in temperate climates, Appl. Energy. 178 (2016) 943–961. doi:http://dx.doi.org/10.1016/j.apenergy.2016.06.107.

[35] F. Favoino, Y. Cascone, L. Bianco, F. Goia, M. Zinzi, M. Overend, V. Serra, M. Perino, Simulating Switchable Glazing with EnergyPlus: An Empirical Validation and Calibration of a Thermotropic Glazing Model, in: Proc. Build. Simul., 2015.

[36] F. Favoino, M. Overend, Q. Jin, The optimal thermo-optical properties and energy saving potential of adaptive glazing technologies, Appl. Energy. 156 (2015) 1–15. doi:10.1016/j.apenergy.2015.05.065.

[37] Nitin Shukla & Jan Kosny. DHFMA Method for Dynamic Thermal Property Measurement of PCM-integrated Building Materials. Curr Sustainable Renewable Energy Rep (2015) 2:41–46

[38] C. Carbonaro, Y. Cascone, S. Fantucci, V. Serra, M. Perino, M. Dutto, Energy Assessment of A Pcm-Embedded Plaster: Embodied Energy Versus Operational Energy, Energy Procedia, Volume 78, 2015, Pages 3210-3215, http://dx.doi.org/10.1016/j.egypro.2015.11.782.

[39] Cascone Y., Perino M., Estimation of the thermal properties of PCMs through inverse modelling. Energy procedia, 78 (2015), 1714 – 1719.

[40] https://www.rubitherm.eu/media/products/datasheets/Techdata_-RT28HC_EN_31052016.PDF/_<accessed 14 May 2017>

[41] https://www.rubitherm.eu/media/products/datasheets/Techdata_-SP26E_EN_02062016.PDF/_<accessed 14 May 2017>

[42] Komerska A, Bianco L, Serra V, Fantucci S, Rosiński M. Experimental Analysis of an External Dynamic Solar Shading Integrating PCMs: First Results, Energy Procedia, 78 (2015), 3452-3457, http://dx.doi.org/10.1016/j.egypro.2015.11.125.

[43] Elarga H, Fantucci S, Serra V, Zecchin R, Benini E. Experimental and numerical analyses on thermal performance of different typologies of PCMs integrated in the roof space, Energy and Buildings. 150 (2017) 546-557. https://doi.org/10.1016/j.enbuild.2017.06.038.

[44] Lam, J.C.; Hui, S.C.M. Sensitivity analysis of energy performance of office buildings. Building and Environment, v. 31, n. 1, p. 27-39, 1996.

Appendix A: EMS objects and program

The temperature of ***Node N*** is acquired by EMS using the object "Sensor", compiled according to the strings here below, where the field "*Output:Variable*" is "*CondFD Surface Temperature Node N*" and the "*Index key name*" is the name of the surface that is made of the construction containing the PCM layer (for the sake of explanation, this surface is called ***Wall_PCM***). This sensor is named, in these sections, ***Node_PCM***, and will be recalled later in the EMS program. Using the nomenclature describe here above, the following lines can be entered in IDF file to create this sensor.

EnergyManagementSystem: *Sensor*,
Node_PCM, ! − *Name*
Wall_PCM, ! − *Output*:*Variable or Output*:*Meter Index Key Name*
CondFD Surface Temperature ***Node N***; ! − *Output*:*Variable or Output*:*Meter Name*

The object "Actuator" is then used, in conjunction with the input object called "*EnergyManagementSystem:ConstructionIndexVariable*" (see below) to link different constructions and allow the swap between the construction with the heating and that with the cooling enthalpy vs. temperature curve. In this object, the "Actuated Component Type" field is "*Surface*", and the "Actuated Component Control Type", which gives the control type, is "*Construction State*". The following lines can be entered in IDF file to create this actuator.

EnergyManagementSystem: *Actuator*,
Wall, ! − *Name*
Wall_PCM, ! − *Actuated Component Unique Name*
Surface, ! − *Actuated Component Type*
Construction State; ! − *Actuated Component Control Type*

Few variables need to be defined in the EMS to allow a smooth execution of the program to be carried out.

First, using the object "*ConstructionIndexVariable*", two variables, named ***H_Wall*** and ***C_Wall***, in this example, need to be defined, identifying the construction with the PCM in heating mode and in cooling mode, respectively (identified by the names ***Plate Wall_H*** and ***Plate Wall_C***). The following lines can be entered in IDF file to create these variables.

EnergyManagementSystem: *ConstructionIndexVariable*,
H_Wall, ! − *Name*
Plate Wall_H; ! − *Construction Object Name*

EnergyManagementSystem: *ConstructionIndexVariable*,
C_Wall, ! − *Name*
Plate Wall_C; ! − *Construction Object Name*

Second, using the object "*GlobalVariable*", to additional variables, named ***Avg_Temp*** and ***Current_Wall*** are created and will be called in the EMS program for checking the state of the heat storage process (heating vs. cooling). The following lines can be entered in IDF file to create this variable.

EnergyManagementSystem: GlobalVariable,
Avg_Temp, ! − *Erl Variable 1 Name*
Current_Wall; ! − *Erl Variable 2 Name*

Third, a trend variable (named ***PCM_Temp_Trend*** in this example) needs to be created by using the object "*EnergyManagementSystem:TrendVariable*". A trend variable is a log of historical values for Erl variables. A trend log is an array that goes back in time, and for this example, the trend variable includes the values of the previous 20 time-steps. The aim of this trend variable, used in combination with the "*@TrendAverage*" function in the EMS program, is to calculate, at the time step *t-1*, the value of the temperature of the PCM node (**Node_PCM**) as the average value of a given number of previous time steps (the given number is called directly in the EMS program and will be described later). This strategy is adopted to obtain a more smooth history of temperature values for the PCM node (node ***N***), since when close to a change between the heating and cooling process (and vice-versa), the numerical solutions of the heat transfer equation can lead to a temperature value that is oscillating around a stable value, for several time-steps. This averaged temperature value will be then used, in the main EMS program, to assess whether the PCM layer is melting or solidifying. The following lines can be entered in IDF file to create the trend variable.

EnergyManagementSystem: TrendVariable,
PCM_Temp_Trend, ! − *Name*
Node_PCM, ! − *EMS Variable Name*
20; ! − *Number of Timesteps to be Logged*

Fourth, an optional output variable (herewith named ***Current_Wall_Status***) can be created to record the current wall construction status and return this characteristic at every time-step for control purpose. Through this variable, it is possible to check that the program is actually swapping from one wall construction to another (and this means from the enthalpy vs. temperature curve for the heating process to the one for the cooling process). The following lines can be entered in IDF file to create the output variable.

EnergyManagementSystem: OutputVariable,
Current_Wall_Status, ! − *Name*
Current_Wall, ! − *EMS Variable Name*
Averaged, ! − *Type of Data in Variable*
ZoneTimestep; ! − *Update Frequency*

After variables initializations, the focus can be moved to the EMS program (herewith called **EMS PCM Code**) which is first introduced through the object "*ProgramCallingManager*". Through this object, the execution of the program is set to occur after EMS calling point called "*BeginTimestepBeforePredictor*". This point occurs close to the beginning of each time-step, but before the predictor executes. The term "*Predictor*" refers to the step in *EnergyPlus*™ simulation when all the calculations happen for Zone HVAC. The following lines can be entered in IDF file to define the program calling manager object.

EnergyManagementSystem: *ProgramCallingManager*,
Hysteresis, ! − *Name*
BeginTimestepBeforePredictor, ! − *EnergyPlus Model Calling Point*
EMS_PCM_Code; ! − *Program Name* 1

Finally, the actual EMS program containing the conditional expressions to select the right enthalpy curve (through the selection of the correspondent "*Construction*") is defined. It is possible to see that the program makes use of the function "*@TrendAverage*", as previously described, to average the value of the temperature of the PCM node (Node N), based on the information stored in the trend variable ***PCM_Temp_Trend***. The "*@TrendAverage*" function is called, in this example, with an index of *12*, meaning that it will return the running average of values of the temperature in the previous last 12 time-steps. This number is arbitrary and depends on several aspects (e.g. time-step of the simulation, heat transfer conditions), so every modeler is free to choose a value that fits best with its specific simulation. The following lines can be entered in IDF file to implement the EMS program.

EnergyManagementSystem: Program,
EMS_PCM_Code, ! − Name
SET ***Avg_Temp*** = @TrendAverage ***PCM_Temp_Trend*** 12, ! − Program Line 1
IF ***Node_PCM*** > ***Avg_Temp***, ! − A5
SET ***Wall*** = ***H_Wall***, ! − A6
ELSEIF Node_PCM < Avg_Temp, ! − A7
SET Wall = C_Wall, ! − A8
ENDIF, ! − A9
SET Current_Wall = Wall; ! − A10

Appendix B: Inter-software comparison

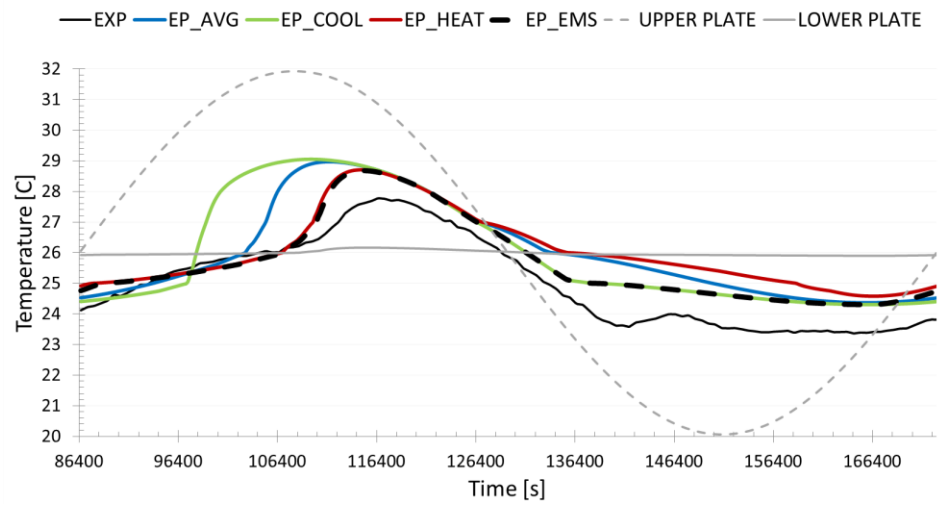

(a)

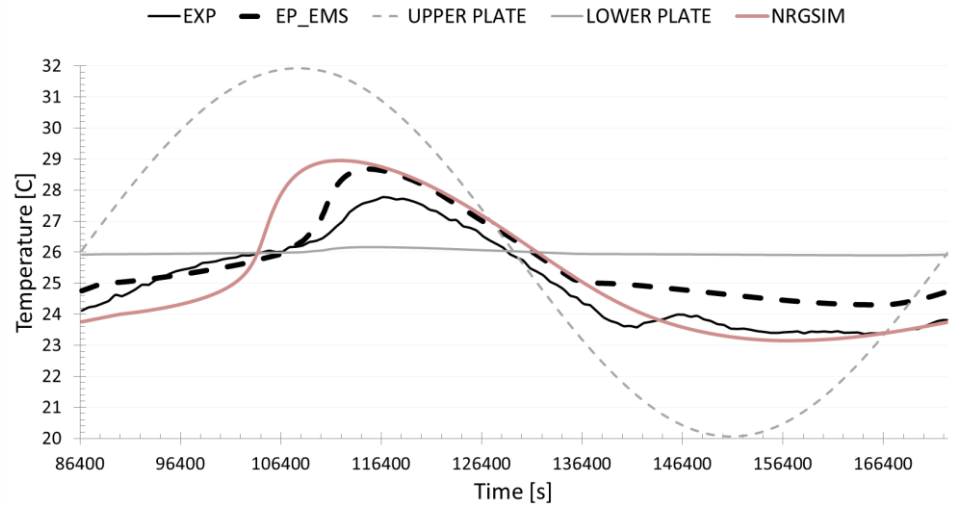

(b)

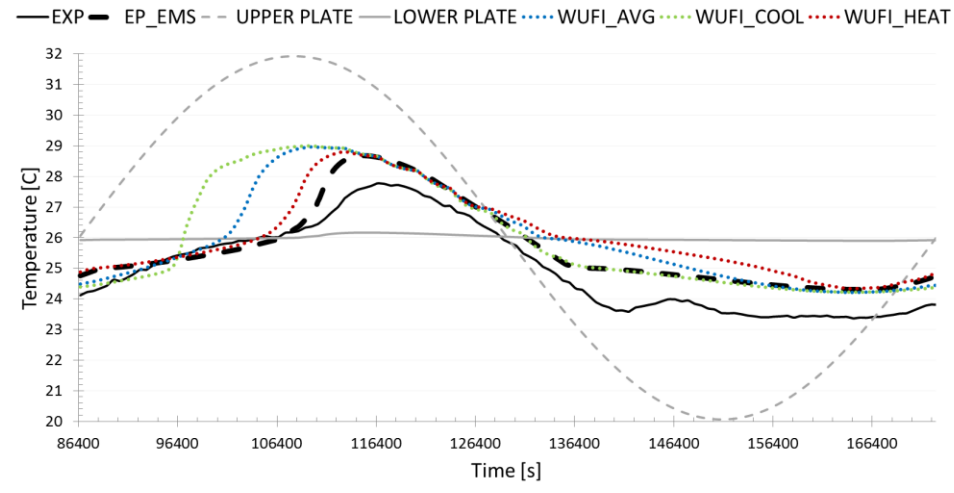

(c)

Figure B.1: *Temperature evolution of* ***SP26E*** *under a stabilized periodic cycle with sinusoidal amplitude of ±6*

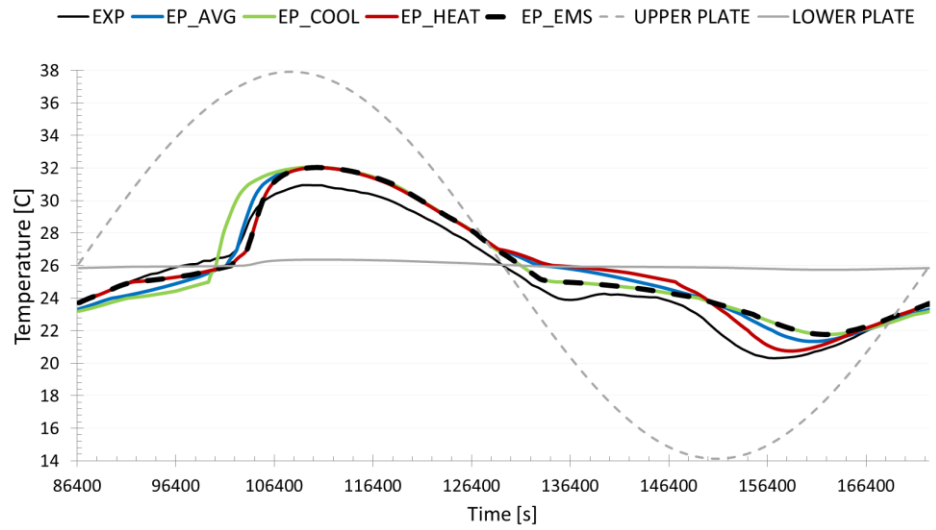

(a)

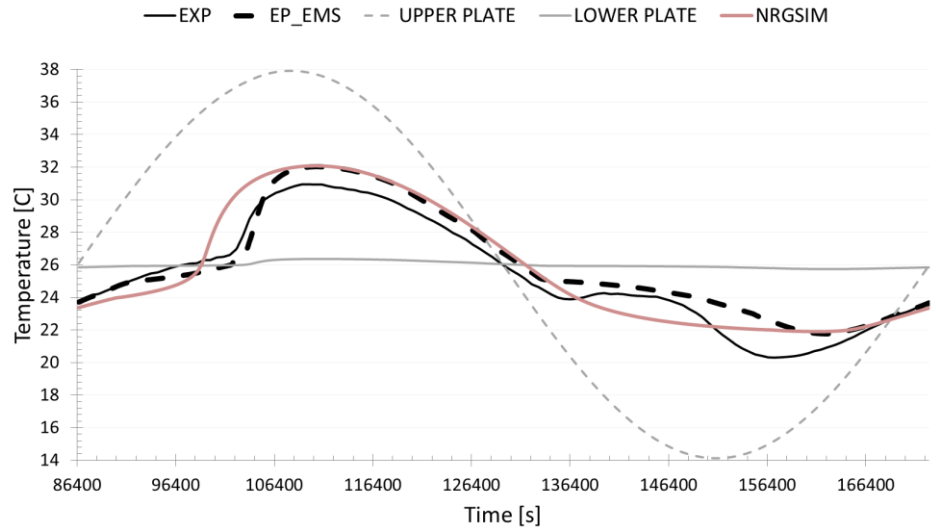

(b)

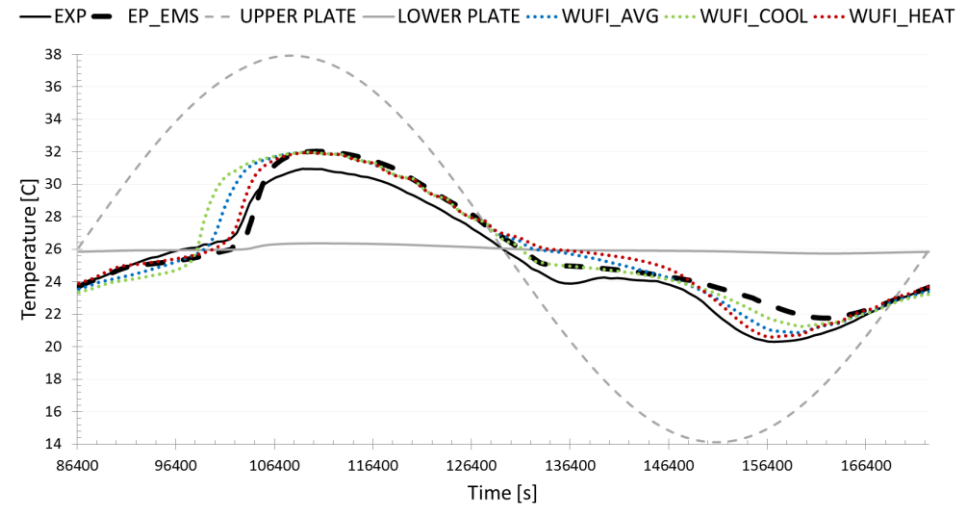

(c)

Figure B.2: *Temperature evolution of* ***SP26E*** *under a stabilized periodic cycle with sinusoidal amplitude of ±12*

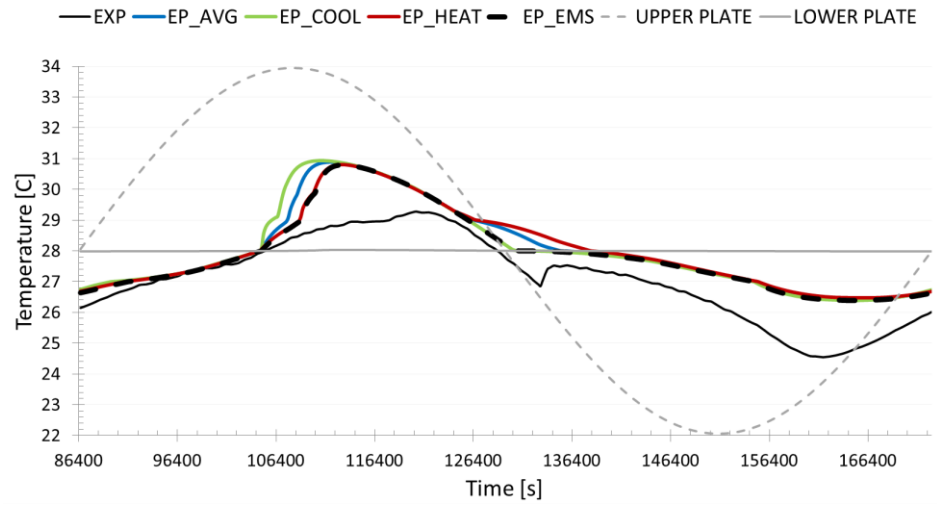

(a)

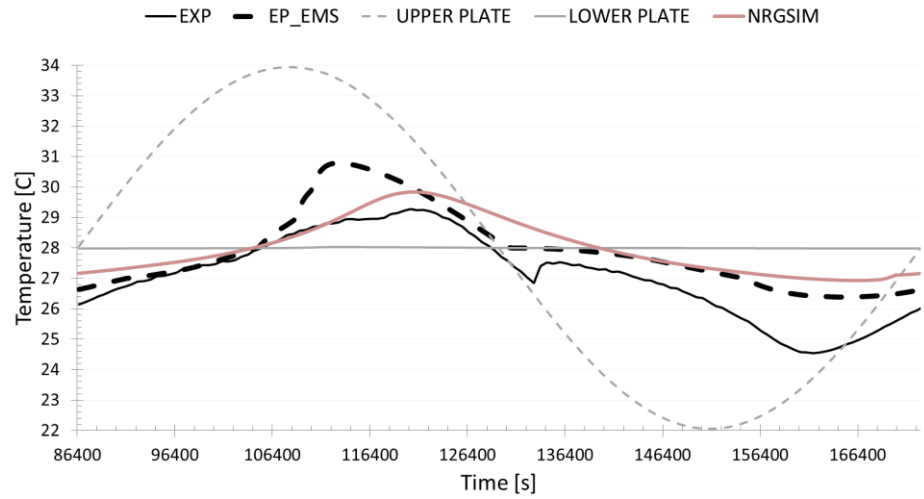

(b)

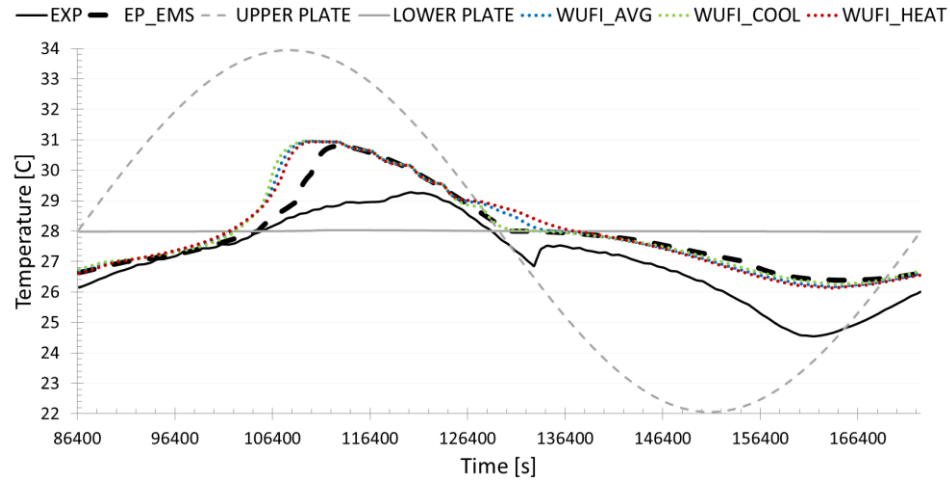

(c)

Figure B.3: *Temperature evolution of* ***RT28HC*** *under a stabilized periodic cycle with sinusoidal amplitude of ±6*

595

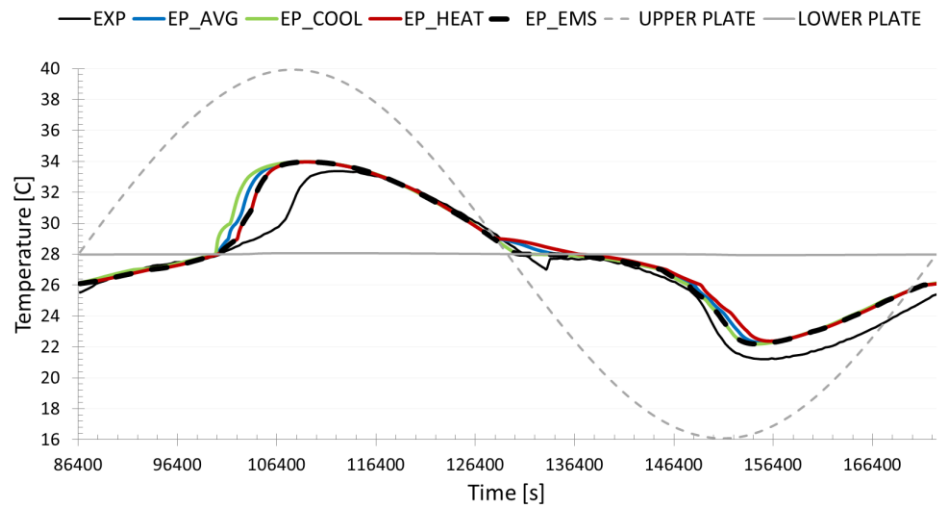

(a)

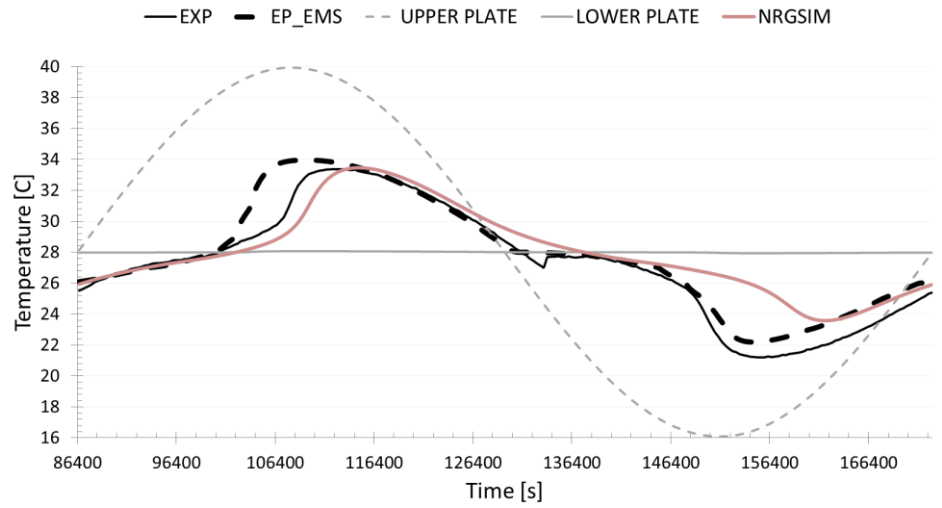

(b)

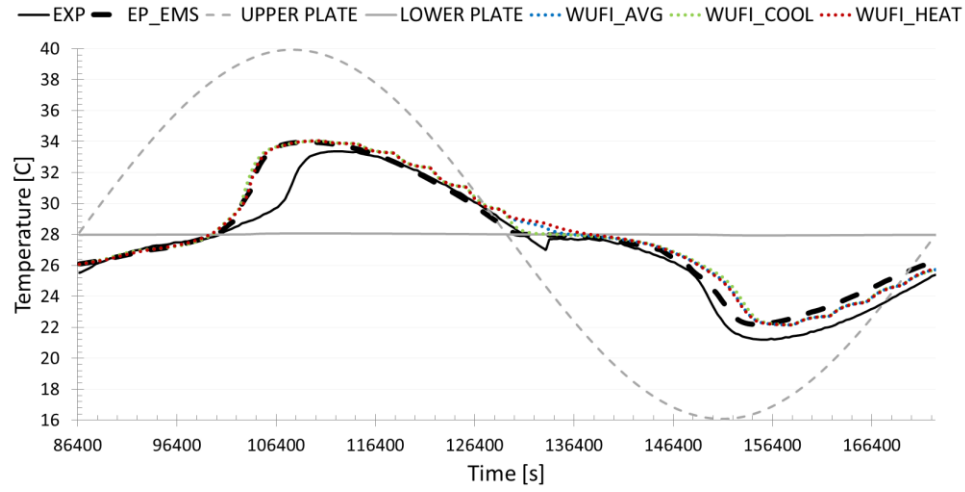

(c)

Figure B.4: *Temperature evolution of* ***RT28HC*** *under a stabilized periodic cycle with sinusoidal amplitude of ±12*

596